UNIVERSITI PUTRA MALAYSIA

PSYCHOPHYSICAL EVALUATION OF CT BRAIN IMAGE QUALITY

MUHAMMAD NUWAIR BIN MOHD ARIF

PSYCHOPHYSICAL EVALUATION OF CT BRAIN IMAGE QUALITY

BY

MUHAMMAD NUWAIR BIN MOHD ARIF

196205

Thesis Submitted to the Department of Physics, Universiti Putra Malaysia, in partial Fulfilment of the Requirements for the Degree of Bachelor of Science with Honours in Instrumentation Science

February 2022

DEDICATION

I dedicate my dissertation work to my family and many friends.

A special feeling of gratitude to my loving parents, Mohd Arif and Roslawati whose words of encouragement and push for tenacity ring in my ears. My siblings Nabila, Najwa, Danial and Danish have never left my side and are very special.

I also dedicate this dissertation to my many friends who have supported and cheered me throughout the process through mental and physical whenever I'm feeling down. I will always appreciate all they have done.

ABSTRACT

Psychophysical Evaluation of CT Brain Image Quality

by

Muhammad Nuwair bin Mohd Arif

196205

February 2021

Supervisor: Dr. Muhammad Khalis bin Abdul Karim

Faculty: Faculty of Science

Since its introduction, Computed Tomography (CT) scan has been adapted with more advance technology allowing for quiet with faster acquisition time. However, CT contribute to high dose exposure which led to radiation including cancer risk. Optimization is essential to reduce the exposure but will result in low image quality obtained. Thus, this study aimed at psychophysical evaluation of image quality by adopting different acquisition setting from the standard protocol. Head-based water phantom was scanned on a 64-slice CT scanner (Canon Acquilion, Japan) with various acquisition CT brain protocol where there are eight protocols named from P1 to P8 and P1 as the standard protocol. The kilovoltage at 120 kVp was maintained as it is the clinical value for tube potential. The main focus of parameter changes in this study is on the change of mAs (tube current), AIDR differences (standard, mild, strong), and the 3D sure

exposure (OFF, low dose, standard, high quality). By using imQuest software, noise and contrast dependent spatial resolution with noise power spectra (NPS), signal of mean with standard deviation (SD) and the signal-noise-ratio (SNR) respectively using five circle regions of interest (ROI) with 38.6 mm diameter. The ratio value of each patient protocol determined from the mean value collected from images divided by the mean of P1. Furthermore, the figure of merit (FOM) was measured based on SNR value and dose value ($CTDI_{vol}$) to establish the relationship between image quality and dose exposure. This study found that the choices of IR selection on AIDR 3D and ^{SURE}Exposure 3D combination as parameter changes underestimated the score of standard parameters produced. High Quality option of ^{SURE}Exposure 3D gave the best results in term of SNR and NPS. However, the dose exposure was too high that it recorded an increase value of 52% from standard parameter. Hence, this study allows for a novel evaluation that estimate the relationship between image quality and dose based on AIDR 3D (IR) and ^{SURE}Exposure 3D.

ABSTRAK

Penilaian Psikofizikal Terhadap Kualiti Imej Otak CT

oleh

Muhammad Nuwair bin Mohd Arif

196205

Februari 2021

Penyelia: Dr. Muhammad Khalis bin Abdul Karim

Fakulti: Fakulti Sains

Sejak diperkenalkan, imbasan Tomografi Berkomputer (CT) telah diadaptasi dengan teknologi yang lebih maju membolehkan ia berfungsi lebih senyap dengan masa pemprosesan yang lebih pantas. Walau bagaimanapun, CT menyumbang kepada pendedahan dos yang tinggi secara tidak langsung membawa kepada radiasi termasuk risiko kanser. Pengoptimuman adalah penting untuk mengurangkan pendedahan terhadap radiasi tetapi akan menghasilkan kualiti imej yang rendah. Oleh itu, kajian ini bertujuan untuk menilai kualiti imej secara psikofizik dengan menggunakan lapan tetapan yang berbeza daripada protokol standard. Fantom air berasaskan kepala telah diimbas pada pengimbas CT *64-slice* (Canon Acquilion, Jepun) dengan pelbagai protokol otak CT pemerolehan di mana terdapat lapan protokol dinamakan dari P1 hingga P8 dan P1 sebagai protokol standard. Kilovoltan pada 120 kVp dikekalkan kerana ia adalah nilai klinikal

untuk tiub potensi. Fokus utama perubahan parameter dalam kajian ini adalah pada perubahan mA (tiub arus), perbezaan AIDR (standard, ringan, kuat), dan ^{SURE}EXPOSURE 3D (OFF, dos rendah, standard, kualiti tinggi). Dengan menggunakan perisian imQuest, *noise* imej, resolusi spatial dengan kontras berserta spektrum kuasa hingar (NPS), isyarat min dengan sisihan piawai (SD) dan nisbah isyarat-*noise* (SNR) masing-masing menggunakan lima kawasan bulatan analisa (ROI) dengan diameter 38.6 mm. Nilai nisbah bagi setiap protokol pesakit ditentukan daripada nilai min yang dikumpul daripada imej protokol P2 – P8 dibahagikan dengan min P1. Tambahan pula, angka merit (FOM) diukur berdasarkan nilai SNR dan nilai dos ($CTDI_{vol}$) untuk mewujudkan hubungan antara kualiti imej dan pendedahan dos. Kajian ini mendapati bahawa pilihan pemilihan IR pada gabungan AIDR 3D dan ^{SURE}Exposure 3D sebagai perubahan parameter menghasilkan skor parameter yang dibandingkan dengan skor parameter P1. Pilihan Kualiti Tinggi ^{SURE}Exposure 3D memberikan hasil terbaik dari segi SNR dan NPS. Walau bagaimanapun, pendedahan dos adalah terlalu tinggi sehingga mencatatkan nilai peningkatan sebanyak 52% daripada parameter standard. Oleh itu, kajian ini membolehkan penilaian baru yang menganggarkan hubungan antara kualiti imej dan dos berdasarkan AIDR 3D (IR) dan ^{SURE}Exposure 3D.

ACKNOWLEDGEMENT

In the name of Allah, the Most Gracious and the Most Merciful.

All praises to Allah and His blessing for the completion of this thesis dissertation. I thank Allah for all the opportunities, trials and strength that have been showered on me to finish writing the thesis. I experienced so much during this process, not only from the academic aspect but also from the aspect of personality. My humblest gratitude to the holy Prophet Muhammad (Peace be upon him) whose way of life has been a continuous guidance for me.

First and foremost, I would like to sincerely thank my supervisor Dr. Muhammad Khalis bin Abdul Karim for his guidance, understanding, patience and most importantly, he has provided positive encouragement and a warm spirit to finish this thesis. It has been a great pleasure and honour to have him as my supervisor.

My deepest gratitude goes to all of my family members. It would not be possible to write this thesis without the support from them. I would like to thank my dearest mother, my father, my sisters and my brothers.

I offer my special thanks to my colleagues; Amir Asyraf, Habibuzzikri, Aliuddin, Hafiz Helmi, Faris and Rahman for the continuous supports until this day since my first-year study as well as my fellow FYP-mates Lokman and Izham. I also want to extend my thanks to Radiologist Staff in the National Cancer Institute, Mr. Shaffiq. And lastly to my seniors Mr. Hanif, Mr. Amirul and Mrs. Aimi for their help. I thank them wholeheartedly.

May God shower the above cited personalities with success and honour in their life.

Table of Contents

LIST OF FIGURES

LIST OF TABLES AND FORMULAS

LIST OF ABBREVIATIONS

CT	Computed Tomography
HU	Hounsfield Unit
ROI	Region of Interest
SNR	Signal-to-Noise Ratio
CNR	Contrast-to-Noise Ratio
MTF	Modulation Transfer Function
TTF	Target Transfer Function
PSF	Point Spread Function
LCD	Low Contrast Detectability
FBP	Filter Back Projection
IR	Iterative Reconstruction
SD	Standard Deviation
kVp	kilovoltage-peak
mAs	Milliamperage-second
QA	Quality Assurance
MPR	multi-planar reconstruction
NPS	Noise Power Spectrum
ALARA	As Low as Reasonably Achievable
ICRP	International Commission on Radiological Protection
IXRPC	International X-ray and Radium Protection Committee

CHAPTER 1

INTRODUCTION

1.1 Background study

CT has been introduced in the last fifty years back on 1971 and since then it has been one of most important instruments in radiographic field alongside Magnetic Resonance Imaging (MRI), ultrasound, and endoscopy. Development of CT technology has been rapid these past few years such helical and multi-slice CT, phase-contrast CT, real-time cardiac CT, micro-CT, and novel detectors such as variable resolution X-ray detectors which can increase image resolution for a better one. Evaluation of images in this study will be deducted quantitatively thus approval testing and quality control of CT scanners are the most important (Allert et al., 2007). Hence, it is importance to diagnose images in high quality available.

Quality assurance (QA) measurements set the aim to control the quality image of CT and dose optimization as in specification measurement and international suggestions. Medical imaging technology widely used as a nondestructive testing also a noncontact method to inspect the anatomy and role of body as well as to detect diseases without damaging test subject's physical. It is stated that medical imaging technology having rapid growth to provide better output of organ's metabolism, and physiology. Medical images give detailed diagnostic, increased visualization, and economical therapies for a disease (Filippou and Tsoumpas 2018).

One of the CT modest in clinical practice is the application of iterative reconstruction (IR) algorithms. IR has the ability to certify the brain image quality at the same dose level as filtered back projection (FBP).

1.2 Problem statement

Ionizing radiation is a radiation that contain so much energy to the level which can affect atoms in living things thus, giving side effect in damaging genetical material such as deoxyribonucleic acid (DNA). Humans are fortunate because this damaged cell can be repaired by their own as long good nutrients is taken care of in daily food consumption. Even so, if the damaged cells are not repaired thoroughly, there are cells that will be dead and in in worse scenario those broken cells turnout being cancerous cells.

Problem that occurred when utilizing (CT) is the risk of exposure to radiation that comes with other side effect. This is due to the dose usage that is high thus increasing the risk on having cancer by the mutation of the DNA (Webb and Henkelman 1990). Hence, World Health Organization (WHO) has classified X-ray as a carcinogen. Human are exposed to vary electromagnetic wave spectrum such as ultraviolet and infrared. Too much exposure to ultraviolet light from sunshine will affect the skin and cause sunburn which will hurt the skin when get in contact. To prevent from such thing happen, sunblock has been developed to cover skin parts that exposed to sunlight and helps to reduce the sunburn pain. Same concept could be applied on CT X-ray which also emit radiation even in small scale. When too much exposure to radiation the risk of getting cancer also will

surge and so the prevention on early stages must be taken. Even though the benefits of X-ray clearly exceed the bad side effect of using them, the precaution steps still need to be executed as one would not know when the bad effect of using X-ray radiation in CT scan technology will take place.

In order to reduce the risk of getting bad side effect on using CT scan, one of the ways that radiologists were likely put their focus is on dropping the dosage they applied on patient which affects the quality of the images to drop (van Ommen et al. 2020). While they likely accepting the low image quality, present-day physicists want to alter and produce the best image quality as possible so that radiologist can have a better evaluation on the outcome print out.

To lessen the quality of the images, there must be a standard set to see how far the quality drop can be contemplated. Thus, this study discusses and evaluates the best parameter with optimized dose level to bring out good image quality for CT brain images.

1.3 Objectives

1.3.1 General Objectives

This study embarks on evaluating the brain image quality of Computed Tomography (CT) scan based on psychophysical measurement.

1.3.2 Specific Objectives

This study is carried out based on the following objectives:

1. To evaluate the CT brain image quality performance by measuring Standard-noise-Ratio (SNR) and Noise Power Spectrum (NPS)
2. To compare the optimized parameter of CT brain examination with the current standard parameter.
3. To develop optimized protocol for CT brain examination that incorporate psychophysical measurement.

1.4 Scope of Study

In this study, the Signal-to-Noise (SNR) and Noise Power Spectrum (NPS) of the brain picture were evaluated. To analyze the picture performance, being familiar with CT image quality assessment tools is a must. Psychophysical evaluation was used to determine CT scan image quality during the process of research. Noise can be classified as a physical principle, whereas contrast resolution and spatial resolution are psychophysical principles. The signal-to-noise ratio (SNR), and noise power spectrum are the metrics employed in this study, which were mentioned in the image quality of CT scan.

1.5 Significance of The Study

The research would give data on CT scan image performance in order to evaluate LCDs based on image quality. It also depends on the parameter and the tools that were used to measure it. The image performance of a CT scan is determined by measuring the CT scan's performance using parameters and image reconstruction. Aside from that, the image's features can be obtained influenced by the image reconstruction, data acquisition in CT, SNR, CNR, MTF, and LCD.

1.6 Thesis outline

This study will be conducted to evaluate brain images quality from CT scan from psychophysical measurement via machine learning. Overall study of this proposal paper will be made up of three chapter where the first chapter contain of background study, problem statement, objectives, scope, and the significance of the study.

The literature review in Chapter 2 summarizes the key findings from prior CT scan investigations and image quality assessments. This chapter delves more into the theoretical aspects of the research field. CT scan is both a principle and a method in this idea. The CT imaging technology, reconstruction technique, CT data capture, and picture quality are all factors to consider. Methods and techniques are covered in Chapter 3 of the paper. Chapter 4 is where all the results produced were discussed in depth with all the data and figure. Lastly in chapter 5 this study was concluded and some suggestions for future study was made.

CHAPTER 2

LITERATURE REVIEW

2.1 Introduction

This chapter was focused on the theories that are relevant to this research. The concepts of computed tomography (CT) scans, CT detectors, CT image reconstruction, picture quality, radiomics, and machine learning were all covered in this chapter.

2.2 Computed Tomography (CT) scan

The information from multiple X-rays is combined in a CT scan, also known as a computed axial tomography (CAT) scan, to provide a full depiction of the inside components of the body. CT scans produce two-dimensional images of bodily parts, yet this data can also be used to build three-dimensional images. As shown in Figure 2.1 below, a CT scanner emits a series of narrow beams into the human body as it passes through an arc. When compared to X-ray images, CT scan images are more accurate (Davis et al., 2018). The mechanism of the CT scan, as well as the parameters employed in the CT scan, were further detailed in this section.

Figure 2.1 Image model of a modern CT Scan

2.2.1 History of CT scan

To get high contrast sectional images, CT had reconstructed the attenuated X-rays. This ground-breaking method was first published in the second part of the 1960s and made clinically available in 1972, has given doctors a fresh perspective on the body of the patient's contrast features. CT machines' architecture, along with the detectors' wide-range sensitivity, give a degree of tissue differentiation not found in any other imaging method. The strong imaging potential connected with the potential of viewing slices of the body made CT one of the greatest triumphs in the development of clinical images in the previous century.

Other world researchers accepted Sir Godfrey Hounsfield's invention of medical imaging. He is recognized with being a key contributor to the invention of CT scanners, which the first CT device patents in 1968 and 1972 were received. In this instance, he won

the Nobel Prize in Physiology or Medicine in 1979 (Broder and Preston 2011). All these new capabilities improved diseases diagnosis and led to the discovery of new pathologies or early stages of pathological tissues. The need for improved ways to improve imaging performance and determine doses in patients was established.

After the first generation of quality assurance and dose assessment CT scanners grew, it became clear that patient safety and image consistency were essential. CT vendor development teams are working hard to achieve better spatial resolution, thinner slices, and faster image acquisition and reconstruction algorithms. Medical physicists and other specialists associated with this CT scan imaging were always concerned about radiation doses and dose reduction measures.

2.2.2 Mechanism of CT scan

A rotary table, an X-ray detector, an X-ray source, processing, visualizing, and a data analysis unit for measurement tests constitute a CT device. In theory, CT creates cross-section images by directing a beam of generated photons from specific angle positions through one plane of an object in a single revolution. As X-rays pass through an item, some are absorbed, some are scattered, and some are transmitted. Attenuation refers to the process of reducing the intensity of X-rays by scattering or absorbing just certain X-rays. Surface interactions attenuate X-rays, which are not detected by the X-ray detector. The X-ray detector does not catch X-rays that have been attenuated by surface interactions. The photons transmitted through the object through each angle are stored on the detector

and displayed by the computer, allowing a complete reconstruction of the scanned part to be created.

The translate-rotate approach was used to develop the first-generation CT system. To generate two images in the through-plane direction, two detectors and a narrow X-ray beam were required. For each projection, a linear modification of the X-ray tube and detector was required, followed by a tiny angle (1°) rotation to determine the next projection. The second-generation CT system was introduced based on the same idea as the first-generation CT system, but instead of a single detector, an array of 30 detectors covered a fan angle of 10 degrees. The most common and popular CT scanners today are third-generation scanners.

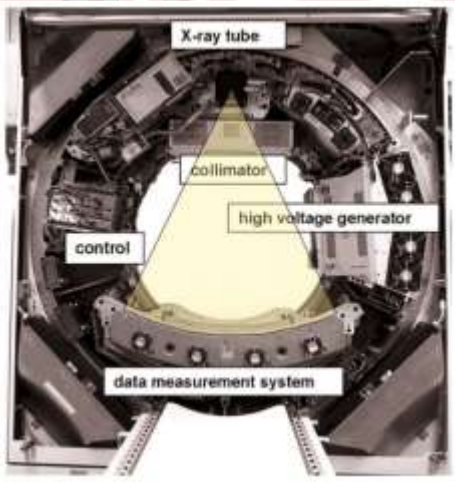

Figure 2.2: Components of modern third generation CT system (Flohr 2013)

As seen in the figure 2.2, they utilized rotate-rotate principle geometry, in which both the detector array and the X-ray tube rotate around the patient. The fan angle detector is around 45-55 degrees, which can cover a large area of body, making this routine more practical. A structure in the body, such as the lung or the liver, may be examined in one breath-hold with little risk of anatomical specifics being revealed. A rotating X-ray tube and a fan beam were used in the fourth generation of CT systems, resulting in a stationary set of detectors that surrounded the patient (Flohr, 2013). These systems had fewer moving parts and did not require signal data to be transferred through a moving gantry. They had the ability to allow the X-ray tube to rotate faster around the patient, reducing the amount of time it took to acquire each slice. The evolution of the first four generations of X-ray CT scanners is represented in Figure 2.3.

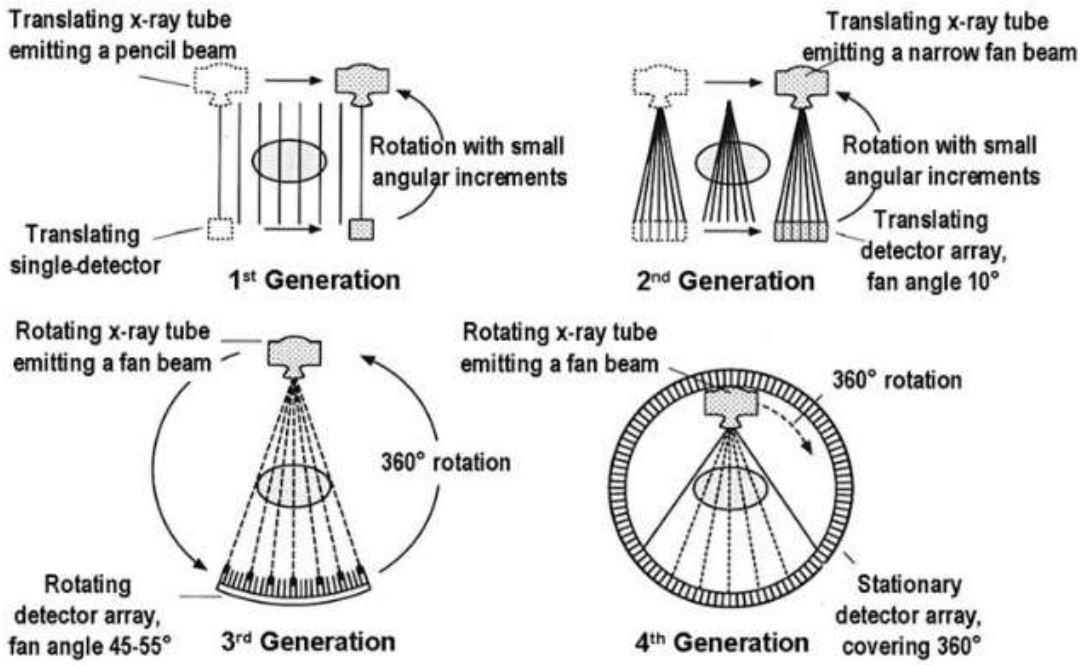

Figure 2.3: Design and acquisition schemes of four generations of CT scanners (Flohr 2013)

2.2.3 CT Detector

Rather than X-ray shadow beam passing through the body part, the CT image is a build-up of cross-sectional view of the patient. The X-rays passed through the object along the various ray pathways that are detected using an X-ray detector. The detector's job is to transform the X-ray incident fluxes into an electrical signal that can be processed using standard electronic procedures.

Gas ionisation detectors and scintillation counter detectors are the two common types of detectors. In the gas ionisation detectors, the incoming X-rays ionise a noble element, which can be in a gaseous or liquid state depend on the pressure. The ionised electrons are accelerated to an anode by an applied voltage, where they form a charge proportionate to the incident signal. The basic procedure for gathering data in CT is visualized in Figure 2.4 below.

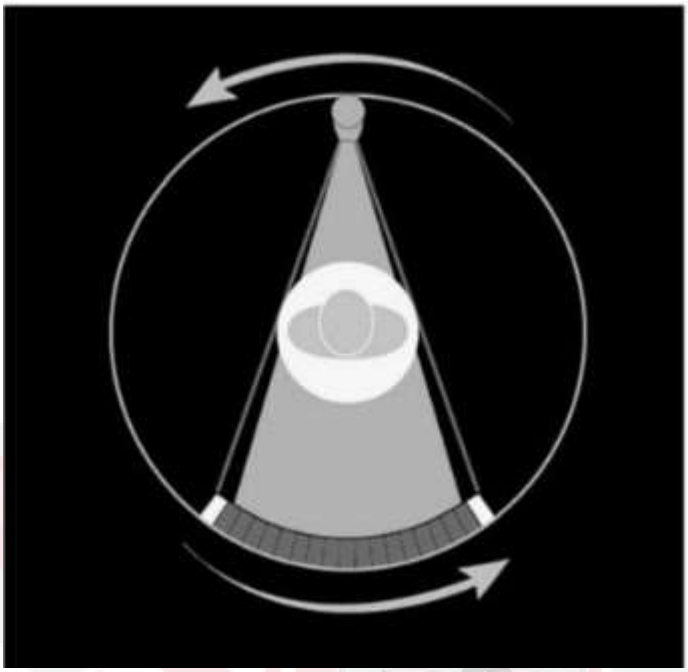

Figure 2.4: Simple CT scan produces a one-dimensional strip radiograph for each projection through the patient.

CT-appropriate sensors can be designed by choosing fluorescent materials that scintillate in proportion to the incident flux and coupling them to some form of device that converts the optical input into an electrical signal.

To construct linear arrays, a single detection system enclosure can be segmented with hundreds of separate sensors. These detectors have been tested with 2MV X-ray sources and are capable of handling higher energy. Scintillator counter detectors rely on the fact that certain materials have the helpful feature of releasing visible radiation when exposed to X-rays. Choosing fluorescent materials that scintillate in proportion to the incident flux and couple them to a device that turns the optical input into an electrical signal to build CT-appropriate sensors.

2.2.4 As Low As Reasonably Achievable (ALARA)

In the field of radiography, the "As Low As Reasonably Achievable" (ALARA) approach is widely applied. The current article gave a historical review of the ALARA principle and its related concepts, as well as their history and development. Meanwhile, the influence of articles on the ALARA concept was mainly unclear (Yeung 2019).

The origin of International Commission on Radiological Protection (ICRP) which was named as The International X-ray and Radium Protection Committee (IXRPC) introduced the danger of overexposure in 1928 thus spread it awareness. In 1950 they establish “as low as practicable” and expand its practicality since 1959 and 1960s. 1966 it was renamed with “as low as is readily achievable” with better understanding and study. Until 1977, ALARA was brought up replacing “as low as is readily achievable” idea and since then the idea was improved to better understanding till these days.

2.3 Image Reconstruction

Image reconstruction is a technique of picture processing in which the spatial domain image data is freed from its representation in the other domains. It is a mathematical method for generating tomographic images from X-ray projection data gathered from various angles around the subject. It has a major impact on image quality and radiation dose as well. For a given radiation dose, image reconstruction with the least noise is preferable without sacrificing image accuracy or spatial resolution. That is

because images of the same quality can be recreated at lower dose levels and image reconstructions that increase image quality can be turned into reduced radiation exposure (Klink et al. 2014). Analytical reconstruction and iterative reconstruction (IR) are the basically two types of reconstruction techniques. Analytical reconstruction can be accomplished using a variety of approaches, where the filtered back projection is the most extensively used way on commercial CT scanners (FBP). Meanwhile, AIDR 3D has been applied for iterative reconstruction. The goal of CT image reconstruction is to figure out how much a narrow X-ray beam can attenuate in each of the reconstruction matrix's voxels.

2.3.1 Filtered Back Projection (FBP)

The filtered back project (FBP) is an analytical reconstruction algorithm developed to overcome the drawbacks of the traditional back project. The image is blurred; therefore, it utilizes a convolution filter to fix it. This method's popularity stems mostly from its computational efficiency and numerical stability. For several generations of FBP-type analytical reconstruction CT data acquisition geometries have been developed, ranging from 2D parallel and fan-beam CT to multi-slice CT with a wide detector coverage (Andersen, Völgyes, and Martinsen 2018). 3D weighted FBP method are usually used on scanners with more than 16 detector rows. Clinical use of CT scanners often has limited influence over the inner workings of the reconstruction process and are only able to alter a few factors that may affect image quality. Noise and streak artifacts are the two major drawbacks of back projection. The iterative algorithm is gradually replacing the filtered back projection image reconstruction technique as the result of combination of these constraints and advancement of computers.

2.3.2 Iterative Reconstruction

Iterative reconstruction is a CT image reconstruction algorithm that starts with an image assumption and compares it to estimated values in real-time while changing the variables. The capability of early scanners had to be limited in computer technology to perform iterative reconstruction. Image reconstruction approach is currently widely used

because of the enhancement in computer technology over the last decade (Beister, Kolditz, and Kalender 2012). The ability to resolve noise associated with filtered back projection without increasing radiation dose had a significant impact on the computed tomography image reconstruction field.

More advanced techniques utilize possibly the best characteristics of data gathering into the reconstruction process. This yields in higher-quality pictures, allowing the patient to consume less radioactivity and receive a lower radiation dose (Samei and Peck 2019). Most iterative reconstruction techniques make an initial approximation of the reconstructed data, as shown in Figure 2.5 below. This could be a uniform image or a filtered back-projected image package. This assumption is used to construct a series of simulated forward projections with the same pixel size and acquisition angles as the real projection data.

Although some data may be limited to reflect the true object due to spatial resolution and noise, the initial projection data received are considered ground reality. This method is repeated or iterated until the desired degree of divergence is achieved. iDose4 is a fourth-generation algorithm that reduces image artefacts and noise while preserving structural and anatomical detail. The use of photon statistics in the projection domain helps to iteratively reduce noise and retain edges, while the use of noise/structure models in the image domain helps to further reduce picture noise. The IRT values utilized in this study were designed to offer a noise reduction factor to compensate for any noise increases caused by the tube output reduction.

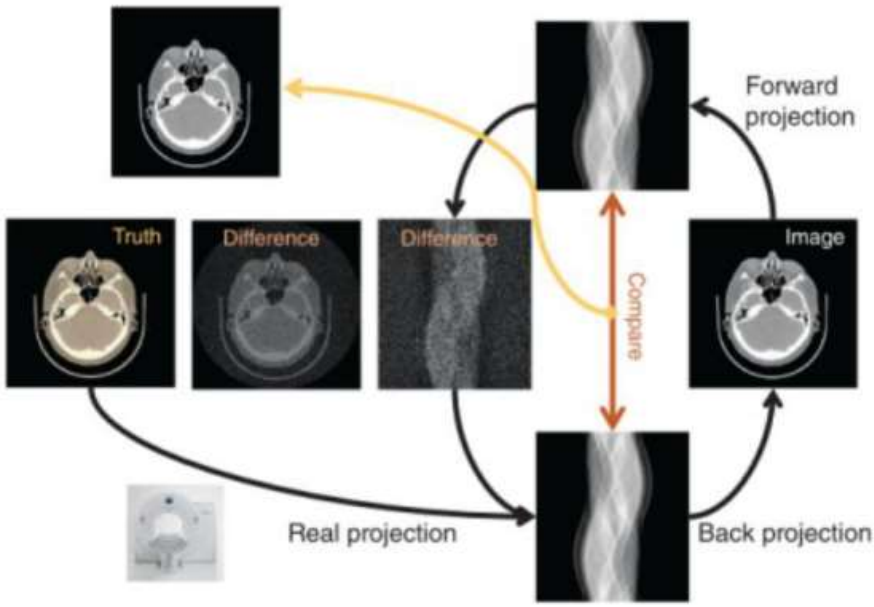

Figure 2.5: Illustration of iterative reconstruction in CT (Samei and Peck 2019)

2.3.3 Adaptive Iterative Dose Reduction 3D (AIDR 3D)

AIDR 3D is an upgraded iterative reconstruction of AIDR that was first introduced in 2010 and the main goal is focusing on dose reduction (Angel 2012). ALARA's guiding philosophy is dose efficiency, which implies getting the best diagnostic picture quality with the least amount of radiation (As Low As Reasonably Achievable). Image quality in CT is defined by the balance of image signal and noise. Picture quality may be improved in two ways: by increasing signal or by lowering the amplitude of image noise compared to the signal. The focus of AIDR was on the second method.

Rather of increasing scanner power or X-ray tube output to boost signal, Aquilion CT reduces noise to reduce dosage. The creation of Adaptive Iterative Dose Reduction 3D (AIDR 3D) was founded on this premise. AIDR 3D is an iterative reconstruction approach that reduces the patient's radiation exposure while minimising the impact on clinical workflow. ALARA imaging is achievable on the Aquilion CT because to revolutionary hardware and software architecture. The advanced reconstruction technique of Aquilion CT is one of its primary distinguishing features. AIDR and AIDR+, the first two phases of iterative reconstruction, involve noise reduction in image space, while AIDR 3D iterative reconstruction, which includes noise reduction in both raw data and image space, is the most recent advancement.

When compared to traditional reconstruction methods, implementing AIDR 3D in a clinical setting is an easy transition because the reconstruction time is swift, there are no additional steps added to the scanning workflow, and image quality is improved while maintaining similar spatial resolution and texture. Dose reduction may very well be performed automatically with an expedited process owing to AIDR 3D's noise reduction and integrated nature. Figure 2.6 below shows the differences of dose exposure value in term of $CTDI_{vol}$, DLP, effective dose and k factor when image scanned without and with AIDR3D.

A.

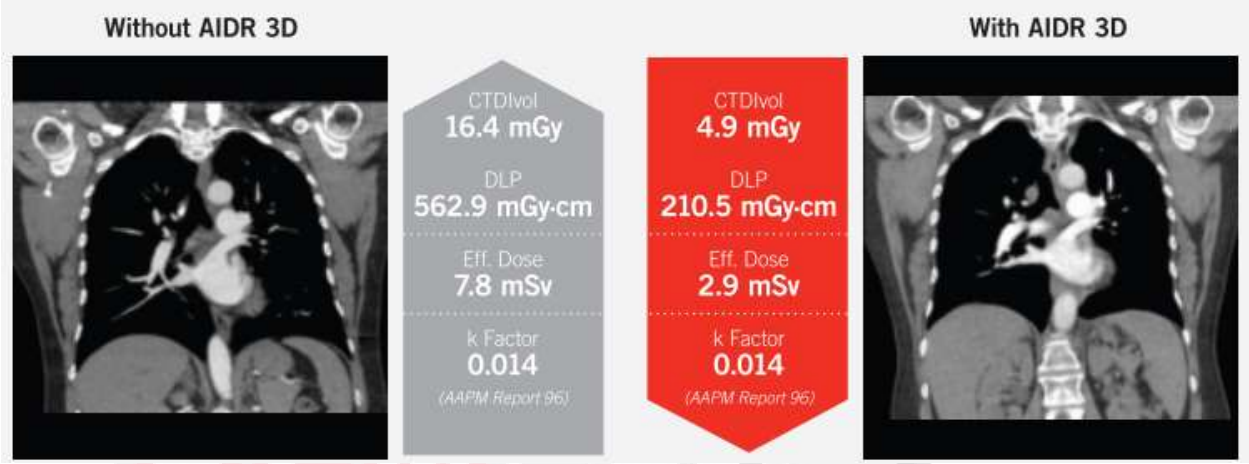

B.

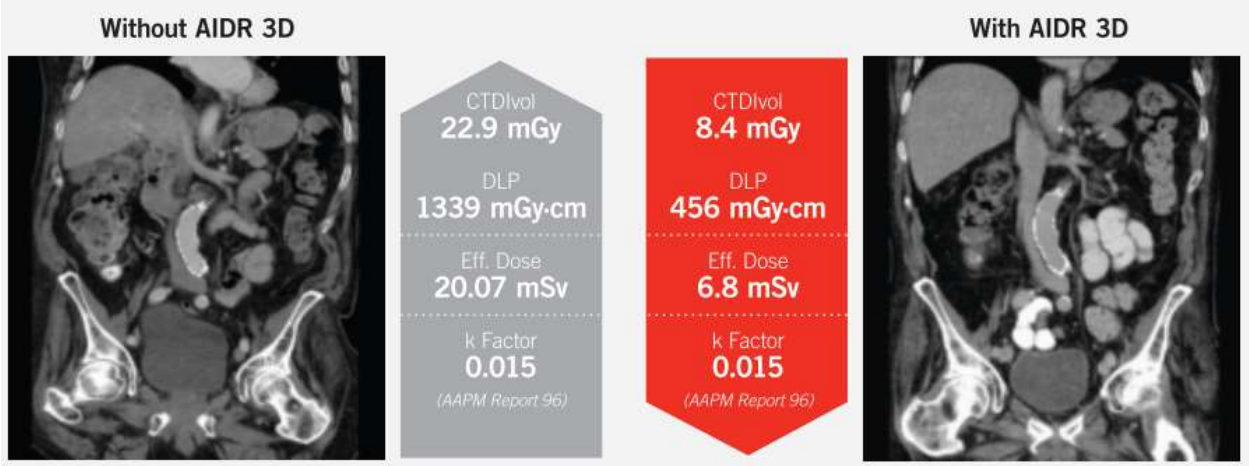

Figure 2.6 A chest CT without AIDR 3D (left) and with AIDR 3D (right) for the same patient.

A. The $CTDI_{vol}$ for the AIDR 3D study was 70% lower than the exam without AIDR 3D

B. Abdomen/Pelvis CT acquired without AIDR 3D with an estimated effective dose of 20 msv (left). The estimated effective dose for the AIDR 3D exam was 6.8 msv; 67% lower than the non-AIDR 3D exam. (Angel 2012)

2.4 Image Quality of CT scan

Image quality evaluation in CT is necessary to ensure that diagnostic inquiries are answered correctly while keeping the patient's radiation exposure as low as possible. Individual aspects of image quality are evaluated as part of quality assurance (QA) in the medical field of X-ray instruments. It is essential to clarify the standards for radiation protection in diagnostic radiography in this aspect. When the image quality allows answering the clinical question while keeping the radiation dose as low as possible, the CT examination is said to be optimised (Verdun 2018).

2.4.1 Contrast-to-noise Ratio (CNR)

The CNR metric is a noise estimate in the image that is used to quantify contrast reduction. Both numerical and psychophysical research are made simpler with the CTP600 module. For numerical evaluation, the contrast-to-noise ratio must be calculated. The ratio of signal intensity differences between two regions of interest and background noise is known as CNR (Desai, Singh, and Valentino 2010). The CNR value will be calculated using the low contrast detectability cylinder from the same Region of Interest (ROI) pixels for each reconstruction.

2.4.2 Signal-to-noise Ratio (SNR)

The signal-to-noise ratio (SNR) is a term used in radiology to describe the ratio of true signal (representing real anatomy) to noise. In medical imaging, SNR is used to characterise image quality. The signal level that provides the SNR threshold is commonly used to establish the sensitivity of an imaging device (digital or film). SNR in CT follows basically the same rules as in standard radiography. It is determined by comparing the target signal's intensity to the background deviation from standard pixel values. In general, the SNR increases as the number of photons transmitted increases (Robinson 2016). In addition, three parameters influence the signal-to-noise ratio in CT: tube current, slice thickness, and patient size. Meanwhile, when the tube current increases, so does the SNR and for the slice thickness; the thicker the slice thickness, the higher the SNR. In terms of the last factor, the signal-to-noise ratio decreases as the patient size increases.

2.4.3 Low Contrast Detectability (LCD)

Low contrast detectability is an important component of X-ray diagnostic imaging systems. A major issue in radiology today is how to lower the dosage of radiation used during CT tests without sacrificing image quality. In general, larger radiation doses can identify smaller objects with poorer contrast, whereas lower radiation doses cause the image having more noise. The risk of cancer triggered by radiation increases when the dose of radiation is raised. In a CT scanner, low contrast resolution refers to the smallest

item that may be detected at a given contrast dose and level (Hernandez-Giron et al. 2015). The contrast level is usually expressed as a percentage of the linear attenuation coefficient of water. With the current approach, a sample specification may be 4 mm at 0.3% contrast for a 10 mm slice thickness at 30 mGy $CTDI_{vol}$ dosage. Other dose measurements, such as the surface dosage measured on the phantom's exterior surface, are also used. A CT system of low contrast detectability (LCD) performance is an important feature that determines the scanner's ability to produce high-quality images with the least amount of X-rays.

2.4.4 Modulation Transfer Function (MTF)

The imaging system that response to the various spatial frequencies in the images is known as the modulation transfer function (MTF). It is a term that is frequently used to describe spatial resolution. The ability to differentiate two separate objects that are directly tied to the pixel dimension, the reconstruction kernel, and the hardware of the imaging instrument is referred to as spatial resolution. The MTF determines how much contrast is retained in the actual object by the detector. The MTF is made up of two components: resolution and contrast. The ability of an imaging system to examine an object in detail is known as resolution, whereas contrast is the lowest or maximum amount of intensity values conveyed from the object to the picture plane. Point Spread Function (PSF) equation also can be used to determine MTF as below:

$$MTF(f) = DFT(PSF(x))$$

PSF denotes the detector's response to an endlessly sharp impulse to the imaging system. Modulation Transfer Function can be determined by differentiating (DFT) the Point Spread Function (PSF), as shown in the equation above. Because it measures the degree of blur and contrast over a variety of spatial frequencies, MTF is a trustworthy parameter for determining effective resolution (Paruccini et al. 2017).

2.4.5 Target Transfer Function (TTF)

The Target Transfer Function (TTF) is a generalization of the Modulation Transfer Function (MTF) (Paruccini et al. 2017). It was created to study the effect of varied levels of contrast on the system's spatial resolution. TTF and MTF are quite similar, however they differ such that MTF is only utilised for a single contrast level, but TTF will present three separate curves at three different contrast levels for a single measurement. When working with non-linear algorithms whose resolution is influenced by contrast, this provides for a resolution characterisation. After that, the Target Transfer Function was assessed in equation below:

$$TTF(f) = DFT(\frac{d(ESF)}{dx})$$

Edge Spread Function (ESF) is described as the system output response to an input edge, according to the AAPM Task Group 233 Report. To compute the value of TTF, differentiate (DFT) the function of ESF with variable x using the equation above.

2.4.6 Noise Power Spectrum (NPS)

While the standard deviation of noise is easy to calculate, it offers no information on the spatial properties of the noise and hence has only a crude predictive value for object detection. As a result, to characterise the noise in this study, the noise power spectrum will be employed. Image noise's amplitude and spatial frequency distribution are both described by the NPS. The noise power variance at each spatial frequency is calculated using the Fourier transform of noise pictures. The degree of randomness at each spatial frequency is reflected in the NPS's magnitude.

The form of the NPS tells where the noise power is concentrated in frequency space: low-frequency noise power concentration implies noise will seem mottled, whereas high-frequency noise power produces finer grain noise (Boedeker and McNitt-Gray 2007). The noise variance is calculated by summing the noise power at all non-zero frequencies in the NPS. The NPS is a more comprehensive noise descriptor than pixel standard deviation since it accounts for both the variance and spatial aspects of picture noise.

2.5 Research Framework on the evaluation of image quality metric of different acquisition protocols

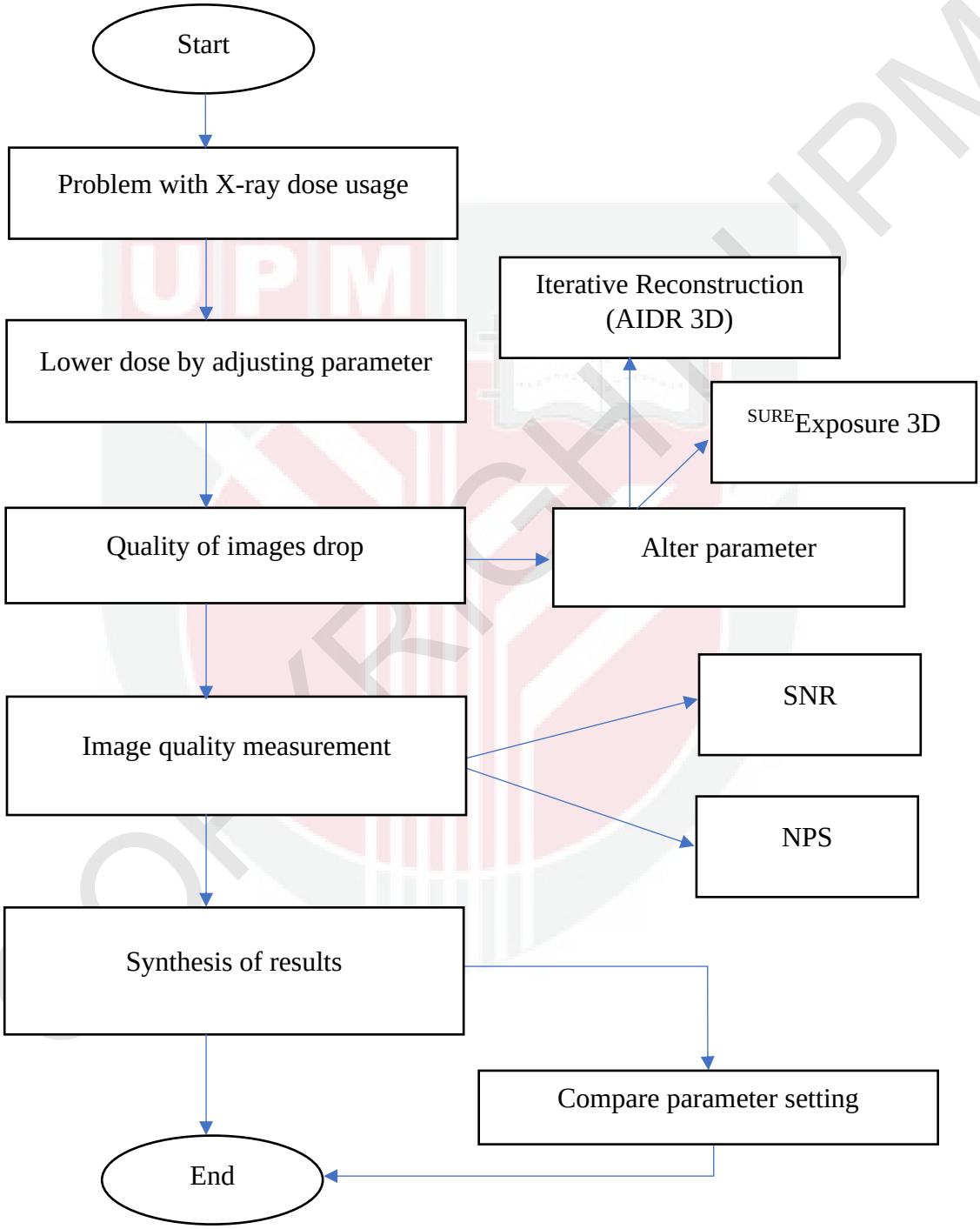

2.6 Summary findings based on the eligible articles of the related study

Year	Author	Title	Finding
2016	Robinson	The Phantoms of Medical and Health Physics	This research covered all sorts of phantoms utilized in medical imaging, treatment, nuclear medicine, and health physics. Dosimetry with regard to material composition, form, and motion/position impacts is all underlined for ionizing radiation. Each sort of medical imaging technology will require specialized materials and designs, and the physics and indications for each type will be investigated.
2017	Völgyes et al.	How Different Iterative and Filtered Back Projection Kernels Affect Computed Tomography Numbers and Low Contrast Detectability	This research stated that computed tomography (CT) numbers and low contrast detectability are affected by different iterative and filtered back projection kernels. In most cases, iterative reconstruction increased contrast-to-noise ratio, but it did so in certain circumstances. For certain densities, there can be significant differences in CT counts amongst kernels of equivalent sharpness.
2018	Davis et al.	Assessment of the variation in CT scanner performance (image quality and Hounsfield units) with scan parameters, for image optimisation in radiotherapy treatment planning	This study identified a mechanism for adjusting scan settings on a CT scanner used for radiation treatment planning and investigated how it affects picture quality and Hounsfield units (HUs). The picture quality metrics were influenced by all of the scan settings that were evaluated. The most critical factors were the reconstruction method, FOV, collimation, and effective mAs. The HU was significantly affected by the reconstruction method and acquisition FOV.
2018	Andersen, Völgyes, and Martinsen	Image quality with iterative reconstruction techniques in CT of the lungs - A phantom study	This study discovered that a wide range of methodologies have been utilised to characterise image quality in CT, ranging from objective measures of physical characteristics to therapeutically task-based approaches like model observer and pure human observer approaches.
2019	Weinman et al.	Dual energy head CT to maintain image quality while reducing dose in pediatric patients	this study found that dual energy CT technology can be utilized to preserve or improve picture quality in pediatric head CT while also lowering radiation exposure. The study compared the dual energy (DE) protocol to the CT head protocol of a helical CT head.

2019	Messaris et al.	Patient dose in brain perfusion imaging using an 80-slice CT system	This study observed at how much radiation patients received throughout a CTP scan, which included an unenhanced brain CT, a brain CT angiography, and a CTP scan. The results are lower than those observed in other research, including those that used CT scanners with more slices.
2020	Conzelmann et al.	Development of a method to create uniform phantoms for task-based assessment of CT image quality Juliane	This research created a specialised approach for creating consistent phantoms for task-based CT image quality evaluation. To make consistent phantoms with low-contrast signals, a cost-effective and versatile technique was created. Access to customised phantoms for task-based picture quality evaluation should be made easier using this way.

CHAPTER 3

METHODOLOGY

3.1 Overview

In this chapter, the methods and lists of equipment for this research were explained further. Previous studies on image quality pf CT scans were used as references to achieve that. Furthermore, this chapter was illustrated and explained every step of this study. The techniques, software and equipment list that used in this study were detailed in further detail in this chapter.

This research study was performed at the Department of Radiology in Institut Kanser Negara (IKN) located in Putrajaya. Toshiba CT Scanner was used to perform the examination on the phantom that already prepared there. Selected part of phantom was chosen to simulate the head part.

3.2 Phantom

This study used phantom whose medium is water also known as water phantom to represent the patient head part to assess the image quality. These phantoms play a crucial role in absolute dosimetry calibration of machine output. Additionally, they allow for the systematic inspection of many essential beam shape properties consisting of symmetry and flatness, as they are effortlessly discovered in a uniform medium. Water also is selected because it's far a dominant element in many forms of tissue, easy in chemical composition, and readily available.

Phantom was held on a holder or stand to make it stand still as in figure 3.1. The phantom was calibrated to ensure it position at the centre by align the external marks on it to the outer laser through X and Y-axis so that the X-ray beams from CT scan strike on phantom equally. the phantom was placed on a holder to secure the position so it would not move when the bed move as it being calibrated and keep stand still.

Figure 3.1 Water phantom placed on holder before calibrated

3.2.1 Water phantom

This water phantom was designed with a cylindrical-shaped water tank made of such as Poly(methyl methacrylate) (PMMA) commonly known as plexiglass (refer phantom of medical and health). Although early water phantoms were fabricated in-residence with particular obligations in mind, they now have become broadly available and employed in recurring scientific use regularly are received commercially. In general, all have comparable creation, with tanks having clear walls fabricated from acrylic, open to the top. The phantom built was 15 cm in diameter and 20 cm in length

3.3 CT Scan

For the use of this study, third generation CT scanner was utilized as it is the most common scanner used nowadays. A considerable improvement was made from 2nd generation CT to 3rd generation CT with a fan-beam shaped X-ray beam capturing all the data (for a slice) within each view, where the translation of source within each image was removed. Because both the X-ray source and the X-ray detector are rotating at the same time, this acquisition mode is called rotate-rotate. The X-ray tube and detector are mounted by using a rigid ring so that they can rotate around the patient. In term of time consuming, third generation CT scanner perform better than the first two generations as it can image the entire part scanned in short time with the isotropic 3-dimensional spatial

resolution. According to the manufacturer, the third generation CT scanner had an enhanced iterative reconstruction approach that reduced image noise (Sandfort et al. 2016).

3.3.1 CT Model

The provided CT scanner in place is a 64-slice CT scanner (Canon Acquilion, Japan) which can perform conveniently without problem as shown in figure 3.2. Scanning time can be done within seconds even for full-body scanning while giving sharp 3D images if requested. This CT-Scanner consists of two command interfaces on both left and right side. It can be access either one to make adjustment on phantom placement. With the help of latest technology advancement, the bed can even hold the maximum weight of 205 kilograms of patient. This machine can utilise its' potential of one full 360º scan time in just 0.35 second.

Figure 3.2 Canon Acquilion 64-slice CT-Scanner made in Japan

3.3.2 CT Protocol

CT protocol is a set of parameters that has been used according to the needs of scanning type. In this study, the routine adult head CT protocol is followed as the standard protocol provided by the CT system there. Thus, the setting was recorded to be compared to the parameter change made. As for this study, two type of parameter was chosen as the variable changed which are the Iterative Reconstruction (IR) and ^{SURE}Exposure. This change parameters variable change affects the other setting such effective mAs because the auto adjustment to bring out the best possible image quality while the others were maintained. Thus, eight patient protocols have been set. Table 3.1 tabulated all eight protocols that was used in this study.

Table 3.1 Protocols comparison with selected changes each on IR and SUREExposure 3D

	Protocols							
Parameter	P1	P2	P3	P4	P5	P6	P7	P8
kVp	120	120	120	120	120	120	120	120
Effective mAs	267	160	89	347	267	267	267	347
Pitch Factor	0.844	0.844	0.844	0.844	0.844	0.844	0.844	0.844
AIDR 3D (IR)	Standard	Standard	Standard	Standard	STRONG	OFF	MILD	OFF
Nhcol (1 × N)	32	32	32	32	32	32	32	32
Slice collimation	0.5 mm	0.5 mm	0.5 mm	0.5 mm	0.5 mm	0.5 mm	0.5 mm	0.5 mm
Filtration setting	Head	Head	Head	Head	Head	Head	Head	Head
Kernel	FC64	FC64	FC64	FC64	FC64	FC64	FC64	FC64
Rotation time	0.75	0.75	0.75	0.75	0.75	0.75	0.75	0.75
mA	300	300 / 166	300 / 96	240	240	240	240	240
SUREExposure 3D	OFF	Standard	Low Dose	High Quality	OFF	OFF	OFF	High Quality
Dose $CTDI_{vol}$ (mGy)	49.2	39.4	23.2	63.6	49.2	49.2	49.2	75.2

3.4 imQuest

As for image quality measurement, imQuest software was bring forward because its ability to measure mean, SD, NPS, TTF, CNR, and detectability from the images taken. It also can measure he CNR directly for the ROI scanned such in figure 3.3 below. This software is a Matlab-based analysis tool that extracts tube current modulation profiles and measures spatial resolution, noise characteristics, and quasi-linear task-based performance. The open source software was designed to work with the ACR and Mercury Phantoms as it main usage, although it may be used with any phantom with equivalent capabilities. (Samei et al. 2019).

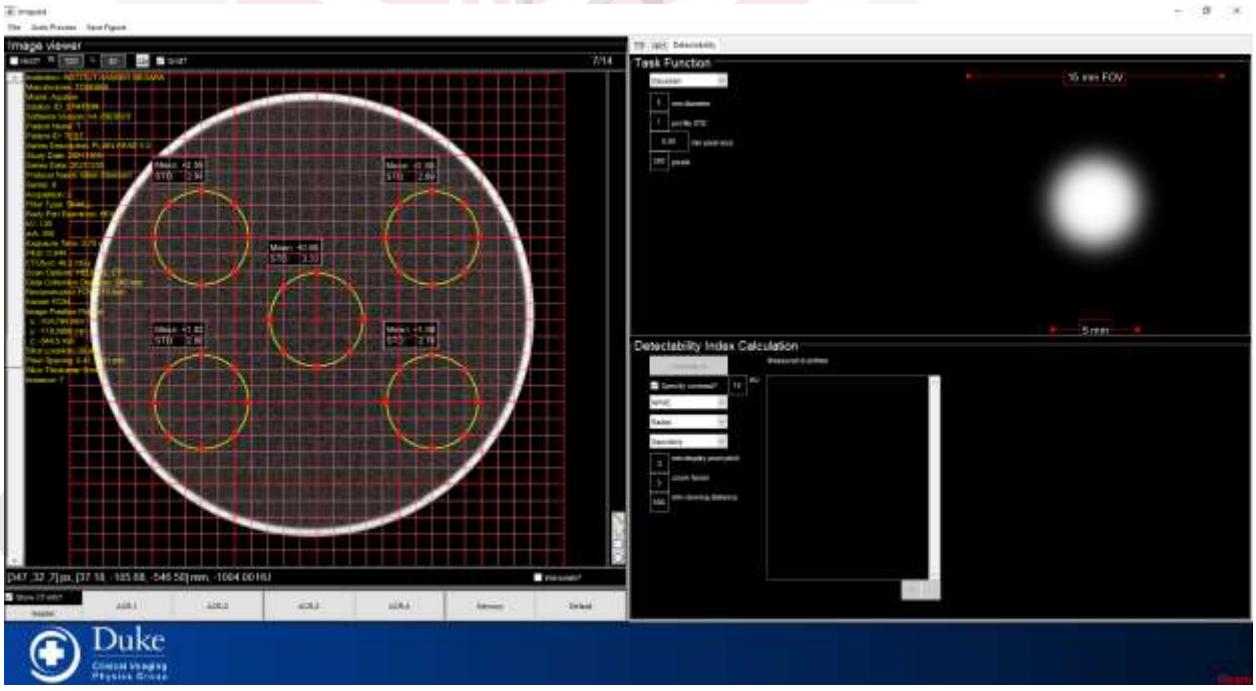

Figure 3.3 Interface of imQuest software built by Samei Group

3.5 Evaluation of Image Quality

Quality of the images in this study was analyse from the measurement of SNR and NPS. A reasonable approach would be that whatever measurement we choose for image quality should at least significantly correspond with the radiologist's definition of high image quality, that is, an image should be of such quality that the radiologist able either to distinguish among various states of disease and health, accurately report diagnostically relevant structures and features, accurately classify different types of abnormalities, or reliably detect relevant structures in the image (M nsson 2000).

Parameters that were monitored and changed were the Iterative Reconstruction and ^{SURE}Exposure. Four different levels of IR were used which are Standard, Mild, Strong, and OFF. As for the ^{SURE}Exposure there were also four type of changes which are Standard, Low Dose, Standard and High Quality. One of these parameters changed while the other parameters kept as constant and vice versa through all the experiment.

3.5.1 Mean and Standard Deviation Assesssment

Mean value was determine from average mean of five ROIs the position of ROIs were consistent at their respective places. To prevent the ROI to vary in places, grid was used as in figure 3.3. For SD, the other name for it is noise but medical physicists used to call it as SD. Value of SD were determined from the same ROIs used for mean value like in figure 3.4.

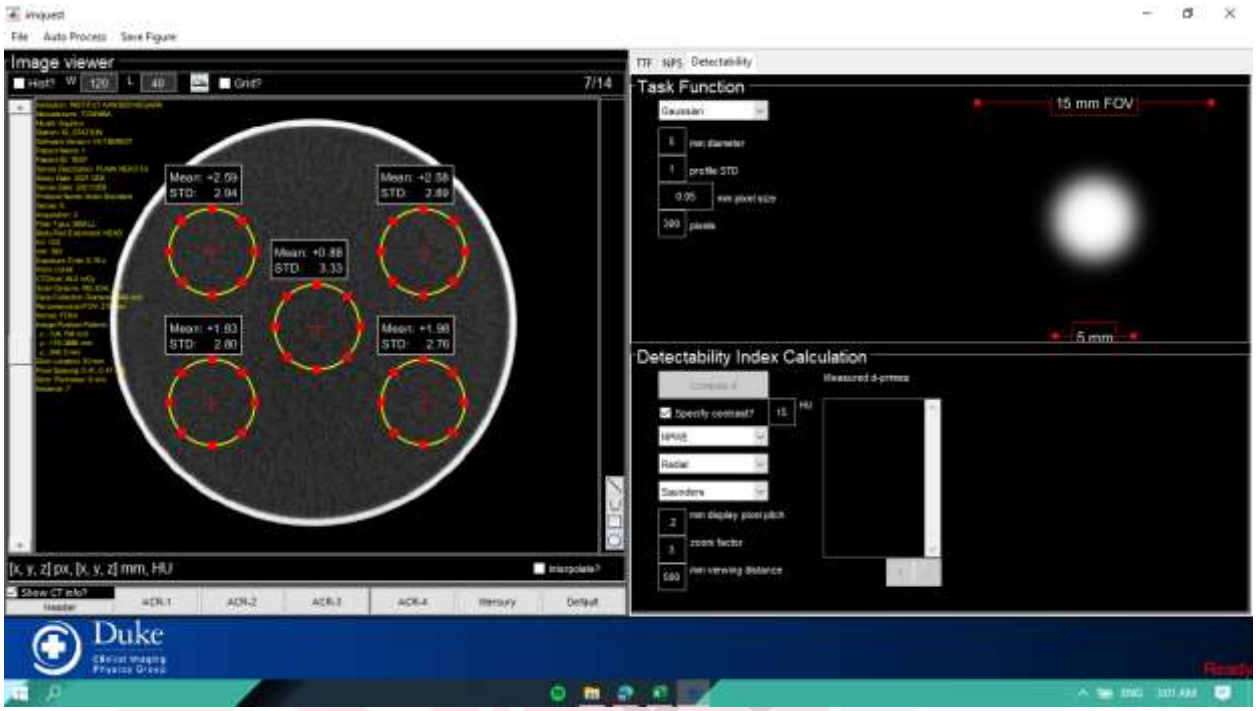

Figure 3.4 Mean and SD ROI placement on same spot throughout all measurement process

3.5.2 Measurement of SNR

Value of SNR was calculated by using the value of mean and SD determined based on equation below (Shaffiq Said Rahmat et al. 2020).

$$SNR = \frac{mean_{ROI}}{SD_{ROI}}$$

3.5.3 NPS Determination

As for NPS value, the measurement was taken using spatial frequency (mm^{-1}) at the graph's highest value or peak value as in figure 3.5. The NPS can be calculated as the Fourier transform of the autocorrelation feature of a synthesised slit in the noise image. However, the NPS is calculated without delay from the Fourier rework of the two-dimensional noise photo. The NPS in this case is the second power of absolutely the value of Fourier transform

In order to get the smoothest curve available, all set of image slices were measured and averaged. Thus, the most accurate NPS line were formed and, in the meantime, reduced the uncertainty (refer paper fourier). This equation was used to calculate the NPS:

$$NPS(f_x, f_y) = c \times [F\{signal(x, y)\}]^2$$

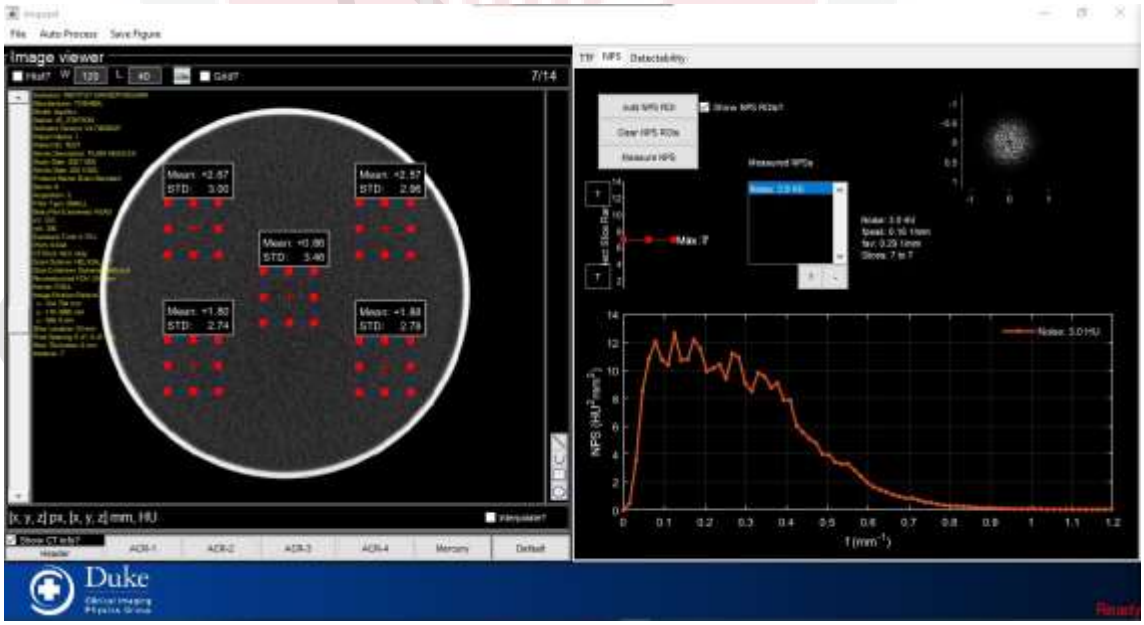

Figure 3.5 NPS measurement with five ROI

3.5.4 Evaluates Spatial Resolution Frequency

Spatial resolution frequency plays a role as to determine which protocol has the best spatial frequency. In the graph built, the best frequency is selected the more it shifted to the right.

3.6 Comparison of Parameter

After all the measurement of SNR and NPS have been done, last step that come is on the differentiation of each parameter. Every change made have been observed and recorded as it is essential in this study to come with the best result among CT protocols made. This part will be discussed further in the next chapter of results and discussion.

CHAPTER 4

RESULTS AND DISCUSSION

4.1 Introduction

In this last chapter, results and data obtained from experiments were analysed and discussed. All results were compared to evaluate which protocol came out with the best image quality. Parameters changed for this were the Iterative Reconstruction and ^{SURE}Exposure 3D. Results shown in this study will be in quantitative measurement. Five different Region of Interest (ROI) was measured for the value of Mean, SD, SNR and NPS for results study shown in figure 4.1.

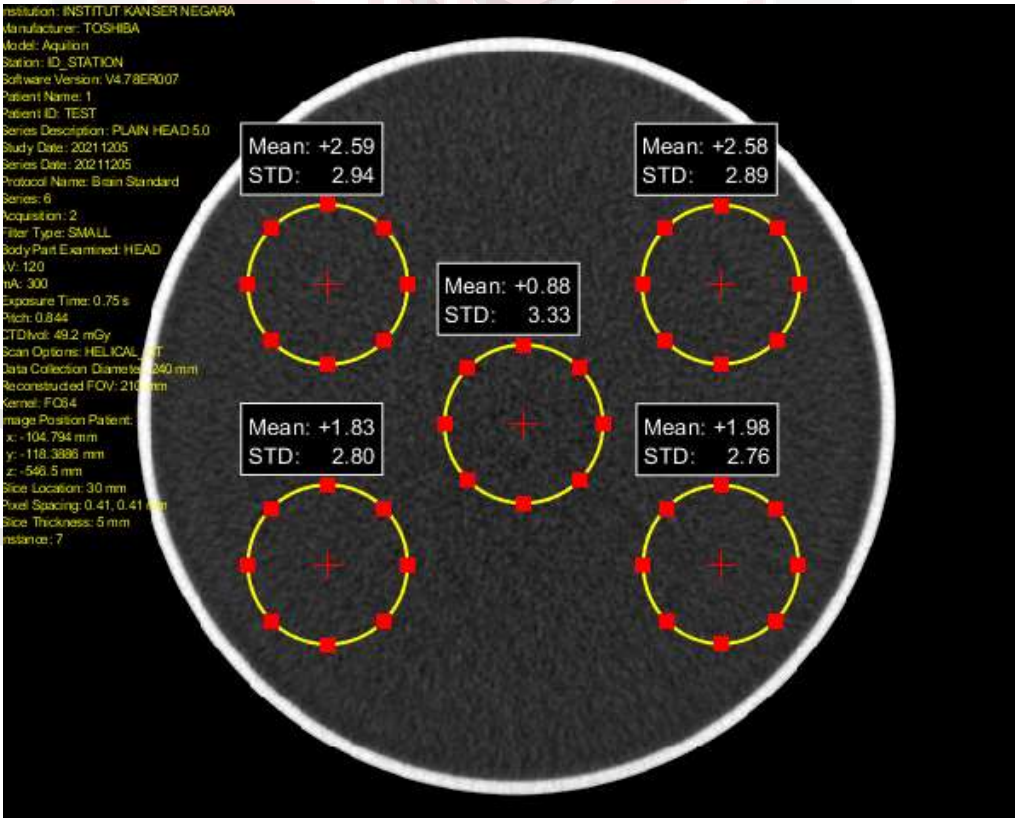

Figure 4.1 Placement of Five ROI studied

4.2 Image Quality Analysis

Based on parameter altered, changes on the SNR and NPS aspect was observed. Based on quantitative analysis, numbers obtained as the results was analysed. The other parameter was set as constant variable such tube potential at 120kVp as it is the clinical value of kilovoltage per peak (refer simple approach to measure CT), pitch factor of 0.844, detector configuration (Nhcol) at 32 mm, slice collimation of 0.5 mm, 5 mm slice thickness and 0.7 second of rotation time. Images analysis was based of the factor that two protocols have been manipulated which is the changes of ^{SURE}Exposure 3D for P1 until P4 while changes of AIDR 3D for P5 to P7 and last protocol of P8 for the mix of protocol changes. All other protocols were made based on the standard protocol which is the P1 provided by the CT scanner system. All the setting involve in this paper study is for the adult patient based.

First step of the image quality analysis is the determination of value of mean and standard deviation or in image study called as noise. As for mean value, it was determined directly from the circle drawn on CT images on every slices. Every protocol produced 14 image slices that was measured to identify every image signal needed to be use on image quality measurement. Every circle area was at the size of 11.702 cm^2 and was kept at matching size for every ROI.

Highest Mean value was recorded on standard protocol which is P1 with 1.972 HU. This shows that the standard protocol already giving out the best measuring signal quality possible. The second highest was P8 which means High Quality option helps in boosting the quality in measuring signal. P5 with 1.87 also classified as one of the highest

since it had Strong AIDR applied. P3 in contrast of using Low Dose SUREExposure 3D had value of 1.836 better than the other 4 protocols. Lowest Mean was recorded on P6 where it turns OFF both IR and SUREExposure 3D setting which fall at 1.72. Mean comparison was pictured in chart form in figure 4.2 and figure 4.4.

The high number in Mean gain does not mean it also had good number in Noise. Figures 4.3 and 4.5 gave the comparison in noise value of all the protocols. P3 was noted with excessive value of Noise with 5.402 hence it was a very bad number. It was noticed even from the observer point of view that the images were grainier than any other images taken. In reflect with P3, P1, P4 and -8 had the lowest Noise value which are 2.944, 2.69 and 2.724 respectively. These three protocols indirectly showed CT images that are smoother with less grain compared to P3. Examples of image to compare the smoothness of P4 compared to P3 was shown in figure 4.6. This was agreed by the other observer when compared the images side by side.

Table 4.1 Mean and Noise value of each protocol

	Measuring Signal						
	HU number	M1	M2	M3	M4	M5	MEAN ± SD
P1	MEAN	0.88	2.58	2.59	1.83	1.98	1.972 ± 0.627
	NOISE	3.33	2.89	2.94	2.8	2.76	2.944 ± 0.203
P2	MEAN	0.7	2.62	2.3	1.45	1.84	1.782 ± 0.672
	NOISE	4.42	3.88	3.92	3.89	3.57	3.936 ± 0.273
P3	MEAN	0.65	2.54	2.5	1.62	1.87	1.836 ± 0.692
	NOISE	6.07	5.25	5.6	5.07	5.02	5.402 ± 0.391
P4	MEAN	0.74	2.53	2.37	1.51	1.99	1.828 ± 0.648
	NOISE	2.99	2.67	2.64	2.64	2.51	2.69 ± 0.160
P5	MEAN	0.79	2.68	2.39	1.51	1.98	1.87 ± 0.669
	NOISE	4.28	3.7	3.71	3.7	3.47	3.772 ± 0.270
P6	MEAN	0.61	2.34	2.31	1.56	1.78	1.72 ± 0.631
	NOISE	4.67	4.04	4.03	3.93	3.81	4.096 ± 0.299
P7	MEAN	0.53	2.43	2.23	1.89	1.79	1.774 ± 0.663
	NOISE	3.71	3.22	3.32	3.14	3.13	3.304 ± 0.214
P8	MEAN	0.79	2.43	2.46	1.8	1.9	1.876 ± 0.606
	NOISE	3.06	2.76	2.69	2.55	2.56	2.724 ± 0.186

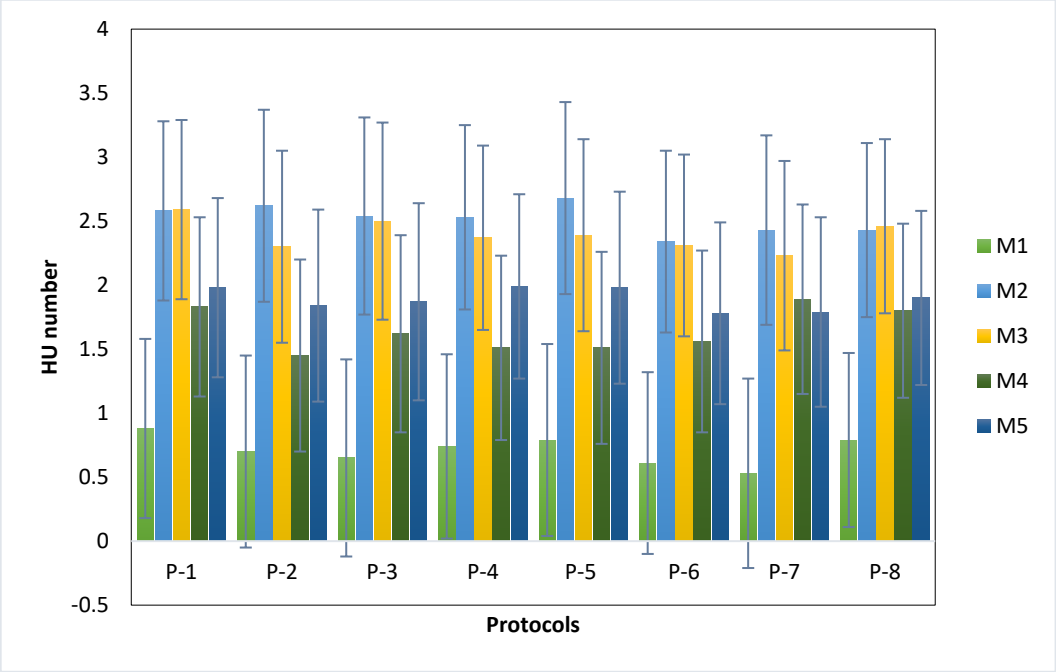

Figure 4.2 HU number of mean every five ROI for all protocol

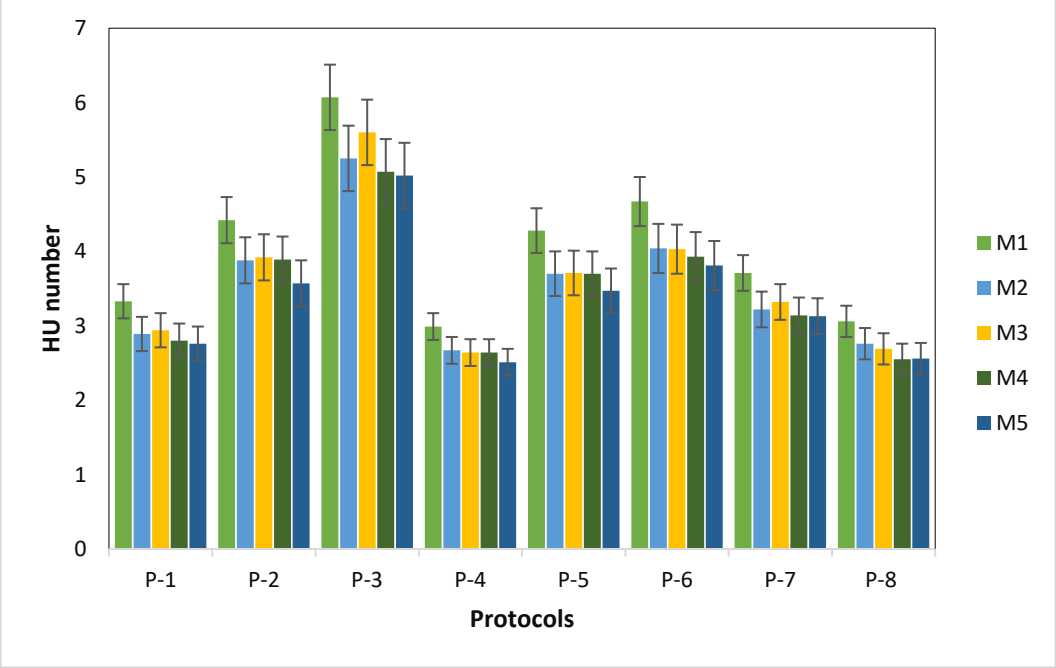

Figure 4.3 HU number of noise every five ROI for all protocol

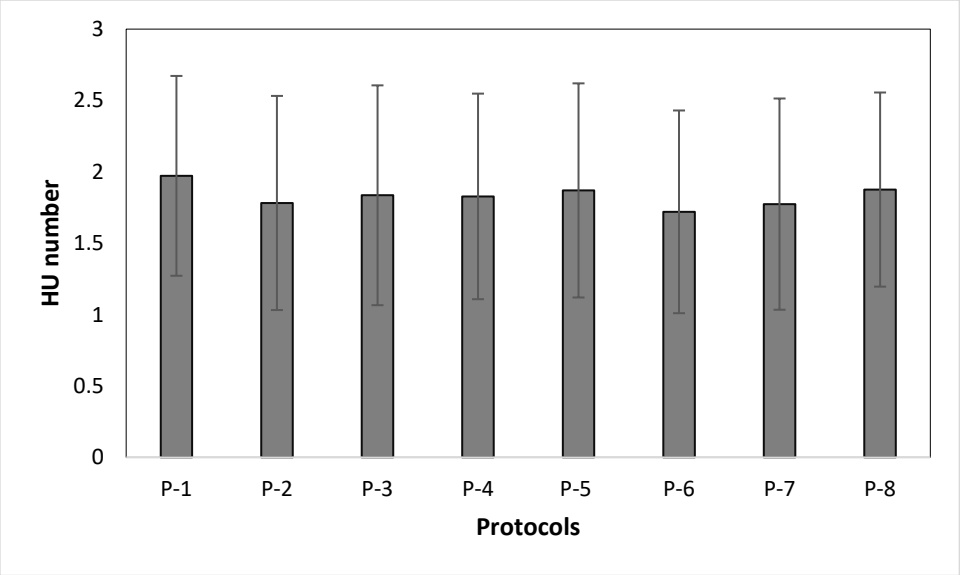

Figure 4.4 Average mean value comparison for all protocol

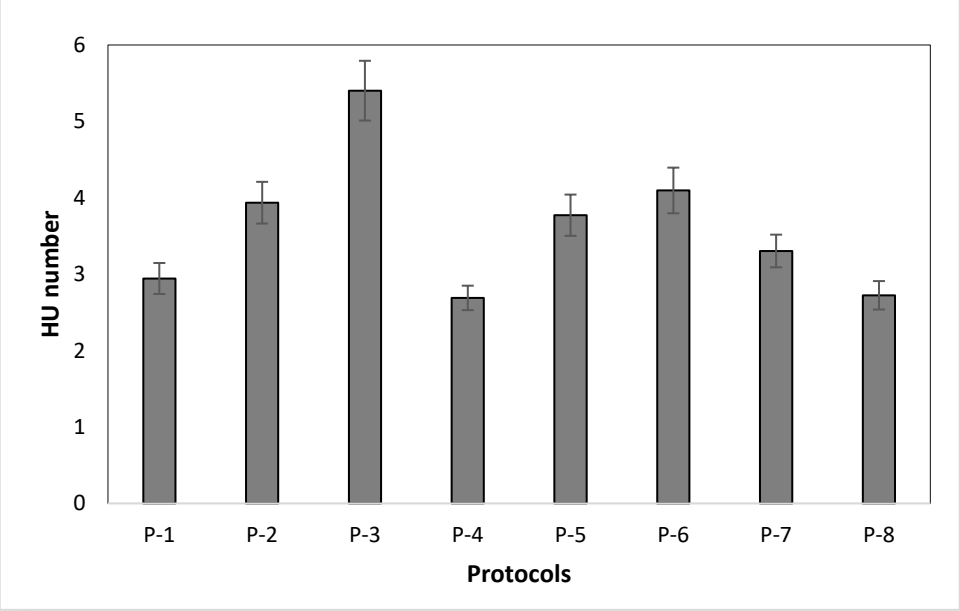

Figure 4.5 Average noise value comparison for all protocol

A.

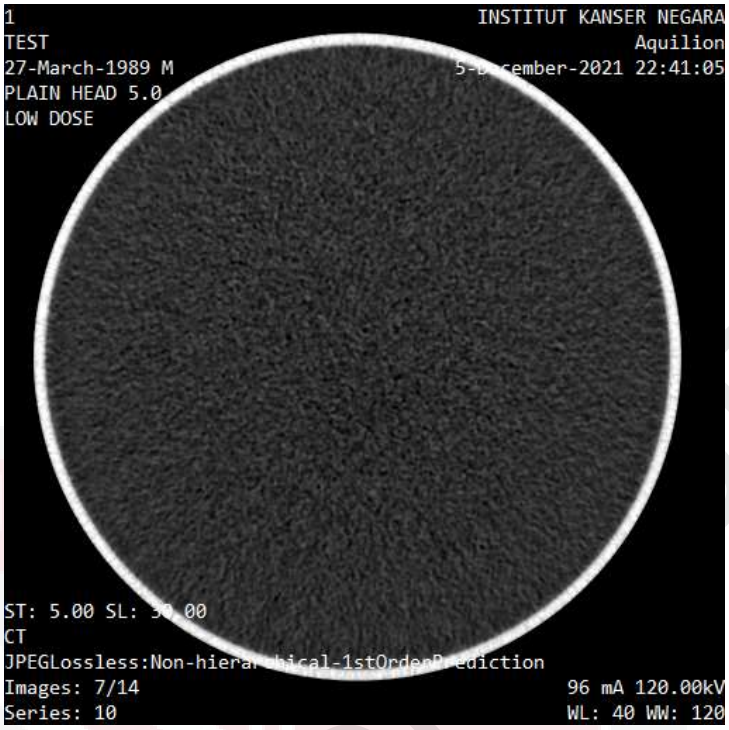

B.

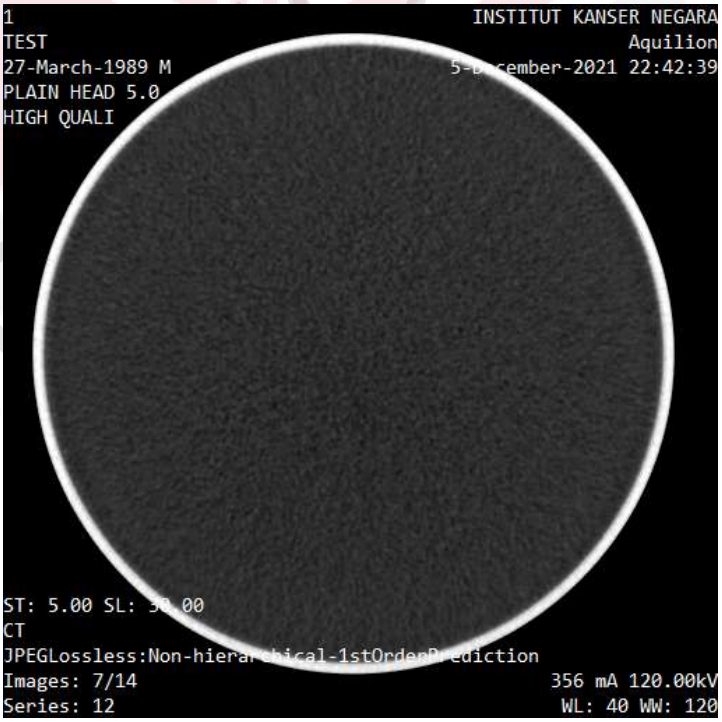

Figure 4.6 **A** image slice of P3 with more noise. **B** image slice of P4 that way smoother.

4.2.1 Ratio Comparison of Changed Protocols and Standard Protocol

Ratio number was determined by dividing average mean value of protocol P2 – P8 with P1 each. Both of mean and noise were used in this ratio measurement. As shown in table 4.2, the value difference also was calculated in percentage to compare how much the changes contrast to the standard protocol of CT brain. Smaller mean percentage which also indicates the value is closer to 1 shows it has good mean produced in the CT images. P5 and P8 were the closest to P1 at 5% differences suggested that both protocols gave good mean signal behind P1. In contrast, P6 had biggest difference percentage thus it gave lower signal than other protocols.

As for noise ratio, P3 was valued at 83% increases in noise value than standard protocol hence it gave an image with more noise even with bare eyes comparison as in figure 4.6. P8 would make a great image protocol because of its ratio was the nearest to the value of 1 with only 7% difference. Therefore, the image slices of P8 came out smoother compared to P3 and other protocols with double digit value of noise percentage difference.

Table 4.2 Ratio of mean and noise with percentage differences

Variables	Protocols							
	P1	P2	P3	P4	P5	P6	P7	P8
mean ratio	1	0.9	0.93	0.927	0.95	0.87	0.9	0.95
difference (%)	0	-10	-7	-7	-5	-13	-10	-5
noise ratio	1	1.34	1.83	0.91	1.28	1.39	1.12	0.93
difference (%0	0	34	83	-9	28	39	12	-7

4.2.2 NPS Evaluation

Noise evaluation did not enough to reflect the images noise for measuring images quality. This is where the need of other type of noise measurement was used to measure it from different perspective. Noise power spectrum (NPS) measurement was evaluated based on spatial frequency (mm^{-1}) at the peak value of NPS and compared in figure 4.8. Surprisingly, the peak value obtained in this study only occurred on two value which are on 0.047 and 0.063 mm^{-1}. These two values turn out to be side by side value which are the fourth and fifth value with differences only 0.015 mm^{-1}.

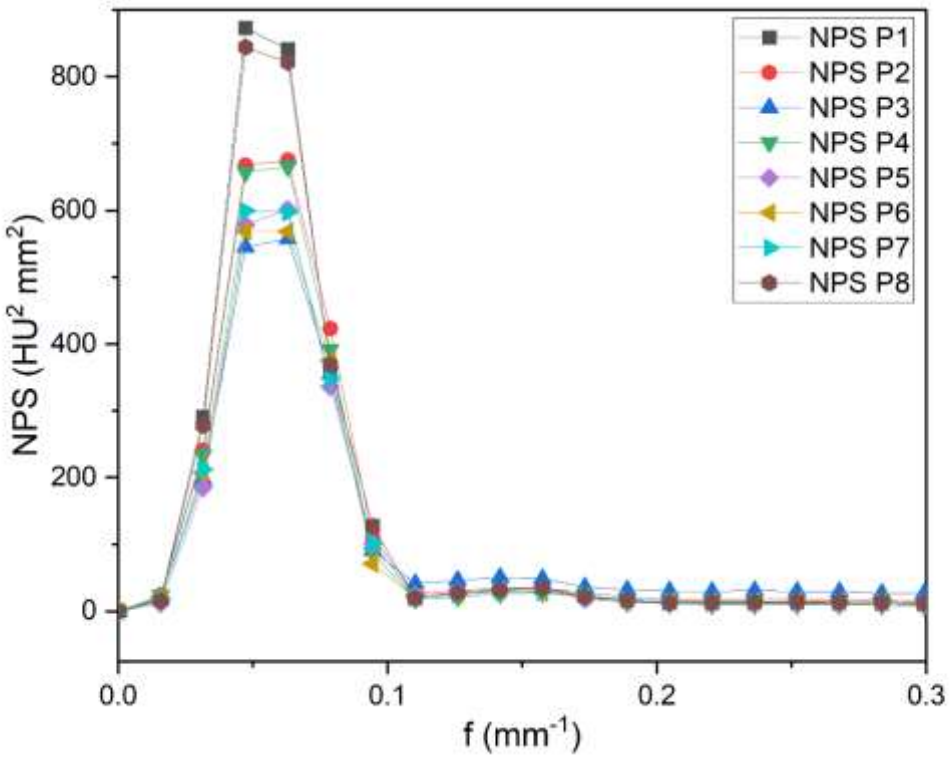

Figure 4.7 All NPS peak value comparison from P1 to P8

From figure 4.9, it shows results from P1 to P4 for the Standard AIDR 3D setting as a constant. SUREExposure 3D was set at different setting for each where NPS peak for P2, P3 and P4 shift to the right on 0.063 mm^{-1} while P1 at 0.043 mm^{-1}. However, even P2, P3 and P4 show better spatial frequency, P1 gave much better NPS result with difference of 200± value. P3 was undeniably giving the lowest NPS because of the Low Dose preference.

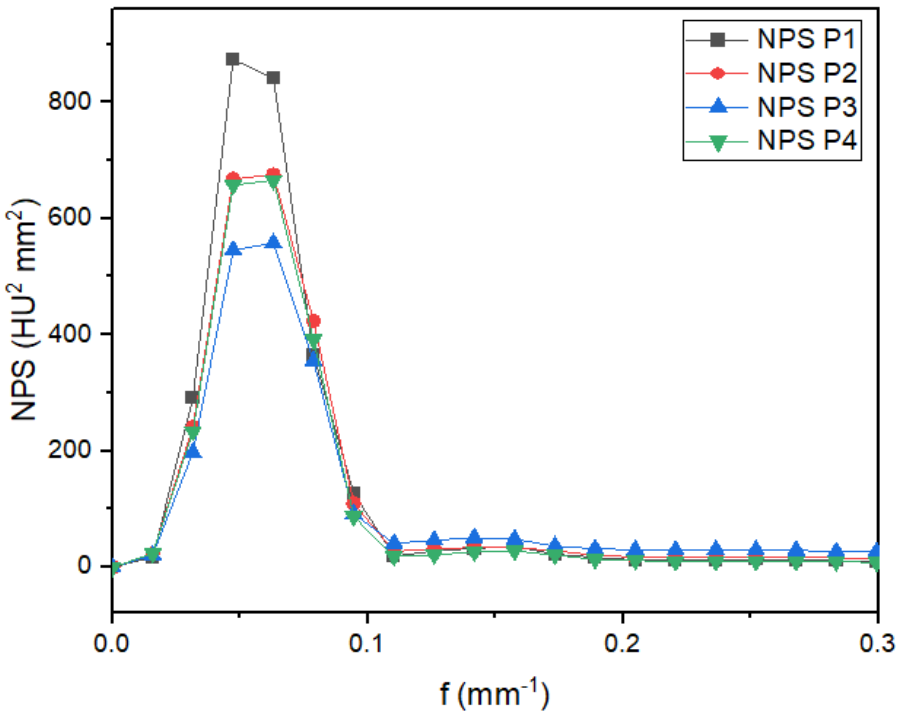

Figure 4.8 NPS peak value of P1 to P4 which is based on standard AIDR 3D

Table 4.3 Results of NPS and SNR of P1 – P4 for different SUREExposure 3D setting

Variable	Protocols			
	P1	P2	P3	P4
NPS peak value (HU)	873.06 ± 2.92	675.08 ± 2.06	557.42 ± 2.29	665.63 ± 2.49
NPS spatial frequency (mm^{-1})	0.047 ± 0.022	0.063 ± 0.013	0.063 ± 0.013	0.063 ± 0.013
SNR	0.68 ± 0.23	0.464 ± 0.18	0.346 ± 0.13	0.692 ± 0.26

From figure 4.10, it shown results of P5 to P7 where it uses constant OFF SUREExposure 3D while changing AIDR 3D setting. P5 placed higher value of spatial frequency and NPS peak value. This shows that Strong AIDR 3D really helps in producing better image quality in term of NPS spatial frequency and NPS peak value. P8 however displays good result where it produces high NPS value at fourth spatial frequency value. P8 only short of 30±NPS value from P1.

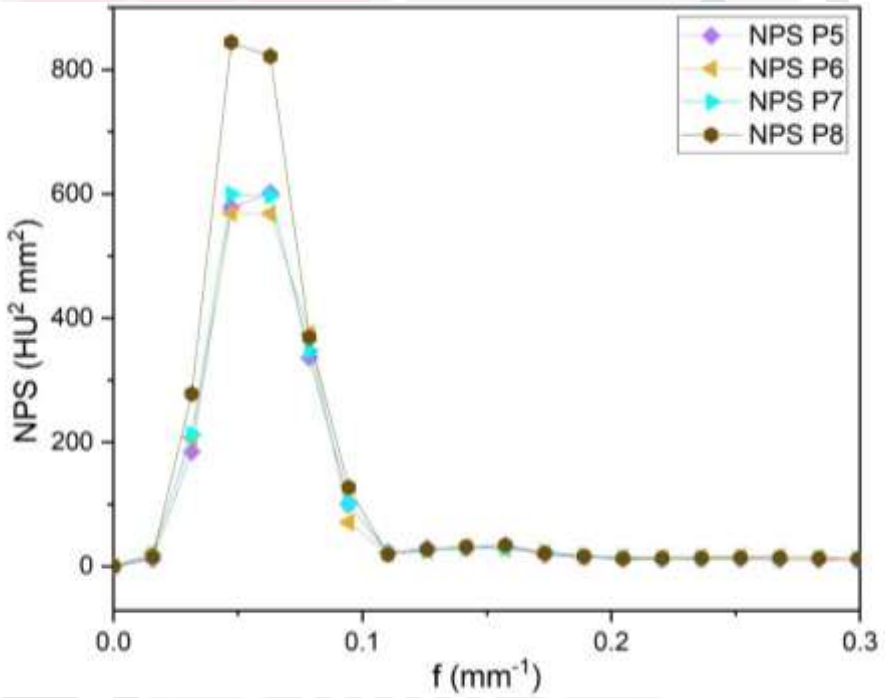

Figure 4.9 NPS peak value P5 to P8 which based on OFF SUREExposure

Table 4.4 Results of NPS and SNR of P5 – P8 for different AIDR 3D setting

Variable	Protocols			
	P5	P6	P7	P8
NPS peak value (HU)	601.22 ± 1.93	569.13 ± 1.57	599.29 ± 1.81	844.34 ± 2.85
NPS spatial frequency (mm^{-1})	0.063 ± 0.013	0.047 ± 0.022	0.047 ± 0.022	0.047 ± 0.022
SNR	0.504 ± 0.19	0.43 ± 0.16	0.546 ± 0.21	0.7 ± 0.23

4.2.3 SNR Assessment

As for SNR, the value was calculated to represent the signal on CT images which means the higher value of SNR, the better it shows the image measuring signal. Results in table show that P8 has the highest value of SNR followed by P4. Both of these protocols used the same setting of SUREExposure 3D of High Quality. The difference of both is that P8 has OFF setting of IR while P4 uses standard setting. Moreover, these two protocols have same value of effective mAs even though the setting is not much same. P4 and P8 are result in higher SNR value than the standard protocol (P1) means that High Quality setting for SUREExposure 3D is producing better signal ratio in term of SNR where P1 uses OFF SUREExposure 3D.

Low Dose SUREExposure 3D as applied on P3 was resulted in the lowest SNR value at 0.35. Low Dose setting in point of fact affects the signal on image produce. Hence, the image quality is very poor and blurry on the eye of observer. P6 was ranked as second lowest SNR value at 0.43 means it also not a good value of SNR for images study either on CT study or patient study. SNR level was compared in chart in figure 4.7.

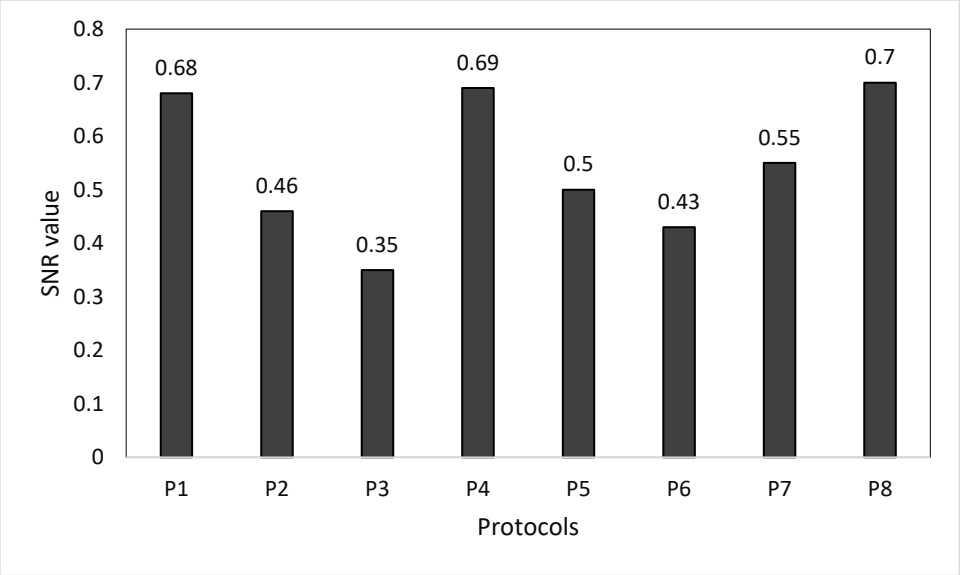

Figure 4.10 Comparison of SNR level for each protocol

4.3 Influence of Optimization

To optimize the CT protocols use on patient of CT scanner, amount of dose absorbed by patient also need to be included in process. By measuring the water phantom, the CT scanner software already provided the amount of doses in $CTDI_{vol}$ for each of protocol. Table show value of $CTDI_{vol}$ for each protocol in unit of mGy. Here shown that P8 with setting of High Quality ^{SURE}Exposure 3D while OFF AIDR 3D produced highest amount of dose exposure. Dose from P4 which is High Quality ^{SURE}Exposure 3D but Standard AIDR 3D, turn out to be the second highest with 63.6 mGy. Here shown that by activating AIDR 3D the dose can be lowered.

Protocols of P1, P5, P6 and P7 gave the same value of dose which are at 49.2 mGy indicate that IR changes did not affect the dose value because of the ^{SURE}Exposure 3D was set at OFF setting. Lowest dose exposure was recorded on P3 where it used Standard AIDR 3D setting with Low Dose set up of ^{SURE}Exposure 3D. It is crystal clear that Low Dose option really helps in reducing the amount of doses applied on patient.

In order to describe the efficiency of dose reduction corresponding to the parameter changed, figure of merit was made. Figure of merit (FOM) is a sum of fraction of image quality over the radiation exposure. FOM was calculated by using the formula below. Best value of FOM was determine on P1 which is the standard protocol setting.

$$\frac{SNR^2}{CTDI_{vol}}$$

Following the ALARA principle, P1 shall be selected as the best protocol to apply on patient then, P4 come after that. P6 shows same dose exposure with P1 however the FOM gain was too low. It was expected because of the low value of SNR it occurred.

Table 4.5 Comparison value of SNR, dose exposure in $CTDI_{vol}$, SNR^2 and FOM

Parameter	Protocols							
	P1	P2	P3	P4	P5	P6	P7	P8
SNR	0.68	0.46	0.35	0.69	0.5	0.43	0.55	0.7
$CTDI_{vol}$ (mGy)	49.2	39.4	23.2	63.6	49.2	49.2	49.2	75.2
SNR^2	.4624	0.2116	0.1225	0.4761	0.25	0.1849	0.3025	0.49
FOM ($\frac{SNR^2}{CTDI_{vol}}$)	9.40	5.37	5.28	7.49	5.08	3.76	6.15	6.52

CHAPTER 5

CONCLUSION

5.1 Conclusion

In this study, CT phantom was utilized for true optimization in clinical practice. The optimization of CT scan protocol is necessary for future use of CT scanner for patient especially for CT brain examination. It has been acknowledged the importance to protect the head from the unnecessary radiation. The overexposure on radiation can effect in brain cells damage thus affecting brain function.

From SNR perspective on this study, P8 should be selected as the best signal provider as it gave the best image signal quality with 0.7. However, P4 and P1 should not be left behind as the result was at very small margin differences where it was recorded at 0.69 and 0.68 respectively. P3 was already expected to be the lowest due to the Low Dose used hence it gave low result.

As for NPS, the NPS spatial frequency and NPS peak value was taken into account in determination of best protocol. There were only two value of spatial frequency which match their NPS peak value respectively. Moreover, these two values were a side-by-side value at fourth and fifth spatial frequency hence it is not a very decent to select on the highest based value which is the fifth at 0.063 alone. NPS peak value was considered, and the highest value was on P1 and P8

To make the optimization aligned with ALARA principle to minimize dose usage, FOM was followed. P1 was selected as the best protocol among other protocols in term of following ALARA. The SNR^2 was ratioed with dose exposure thus showed P1 provided the best result.

This study concluded that the two highest scored protocols were P1 which are the standard setting protocol that uses OFF ^{SURE}Exposure 3D with Standard AIDR 3D and P8 which uses High Quality ^{SURE}Exposure 3D with OFF AIDR 3D. Nevertheless, P8 still underperformed than P1 as the best protocol due to the dose usage that are high at 75.2 mGy while P1 keep it dose exposure at standard rate of 49.2 mGy. Finally, this study experiment to develop a better optimize parameter was not succeed as none of other protocol outscored standard protocol.

5.2 Recommendation for Future Study

From this study experience, recommendation that can be offered is to use a better construct phantom such Catphan® 600 which is a newer phantom and can be studied on more specific part such as fat, soft tissue, air, and bone. Water phantom might get some error with the water used during experiment if the water not being renew.

Different type of IR algorithm can be suggested for future study such as ASIR, SAFIRE, QDS+ and iDOSE to compare each of IR images quality on psychophysical study. Hence the study can decide which IR algorithm is better used.

REFERENCES

Andersen, Hilde Kjernlie, David Völgyes, and Anne Catrine Trægde Martinsen. 2018. "Image Quality with Iterative Reconstruction Techniques in CT of the Lungs—A Phantom Study." *European Journal of Radiology Open* 5 (February): 35–40.

Angel, Erin. 2012. "AIDR 3D Iterative Reconstruction :" *Canon Medical Systems USA, INC*, 0–8.

Beister, Marcel, Daniel Kolditz, and Willi A. Kalender. 2012. "Iterative Reconstruction Methods in X-Ray CT." *Physica Medica* 28 (2): 94–108.

Boedeker, K. L., and M. F. McNitt-Gray. 2007. "Application of the Noise Power Spectrum in Modern Diagnostic MDCT: Part II. Noise Power Spectra and Signal to Noise." *Physics in Medicine and Biology* 52 (14): 4047–61.

Broder, Joshua, and Robert Preston. 2011. "Imaging the Head and Brain." In *Diagnostic Imaging for the Emergency Physician*, 1–45. Elsevier.

Conzelmann, Juliane, Felix Benjamin Schwarz, Bernd Hamm, Michael Scheel, and Paul Jahnke. 2020. "Development of a Method to Create Uniform Phantoms for Task-Based Assessment of CT Image Quality." *Journal of Applied Clinical Medical Physics* 21 (9): 201–8.

Davis, Anne T., Antony L. Palmer, Silvia Pani, and Andrew Nisbet. 2018. "Assessment of the Variation in CT Scanner Performance (Image Quality and Hounsfield Units) with Scan Parameters, for Image Optimisation in Radiotherapy Treatment Planning." *Physica Medica* 45 (November 2017): 198–204.

Desai, Nikunj, Abhinav Singh, and Daniel J. Valentino. 2010. “Practical Evaluation of Image Quality in Computed Radiographic (CR) Imaging Systems.” *Medical Imaging 2010: Physics of Medical Imaging* 7622 (March): 76224Q.

Filippou, Valeria, and Charalampos Tsoumpas. 2018. “Recent Advances on the Development of Phantoms Using 3D Printing for Imaging with CT, MRI, PET, SPECT, and Ultrasound.” *Medical Physics* 45 (9): e740–60.

Flohr, Thomas. 2013. “CT Systems.” *Current Radiology Reports* 1 (1): 52–63.

Hernandez-Giron, I., A. Calzado, J. Geleijns, R. M.S. Joemai, and W. J.H. Veldkamp. 2015. “Low Contrast Detectability Performance of Model Observers Based on CT Phantom Images: KVp Influence.” *Physica Medica* 31 (7): 798–807.

Klink, Thorsten, Verena Obmann, Johannes Heverhagen, Alexander Stork, Gerhard Adam, and Philipp Begemann. 2014. “Reducing CT Radiation Dose with Iterative Reconstruction Algorithms: The Influence of Scan and Reconstruction Parameters on Image Quality and CTDI Vol.” *European Journal of Radiology* 83 (9): 1645–54.

M nsson, L.G. 2000. “Methods for the Evaluation of Image Quality: A Review.” *Radiation Protection Dosimetry* 90 (1): 89–99.

Messaris, Gerasimos A.T., Dimitrios N. Georgakopoulos, Petros Zampakis, Christina P. Kalogeropoulou, Theodoros G. Petsas, and George S. Panayiotakis. 2019. “Patient Dose in Brain Perfusion Imaging Using an 80-Slice CT System.” *Journal of Neuroradiology* 46 (4): 243–47.

n, Eunsung Mouradian, M.Maral. 2008. “Novel Materials for Low-Contrast Phantoms for Computed Tomography.” *NIH Public Access* 23 (1): 1–7.

Ommen, Fasco van, Frans Kauw, Edwin Bennink, Jeremy J. Heit, Dylan N. Wolman, Jan Willem Dankbaar, Hugo W.A.M. de Jong, and Max Wintermark. 2020. “Image Quality of Virtual Monochromatic Reconstructions of Noncontrast CT on a Dual-Source CT Scanner in Adult Patients.” *Academic Radiology*, 1–8.

Paruccini, Nicoletta, Raffaele Villa, Claudia Pasquali, Chiara Spadavecchia, Antonia Baglivi, and Andrea Crespi. 2017a. “Evaluation of a Commercial Model Based Iterative Reconstruction Algorithm in Computed Tomography.” *Physica Medica* 41: 58–70.

“Evaluation of a Commercial Model Based Iterative Reconstruction Algorithm in Computed Tomography.” *Physica Medica* 41: 58–70.

Robinson, Donald. 2016. *The Phantoms of Medical and Health Physics*. *Medical Physics*. Vol. 43.

Samei, Ehsan, Donovan Bakalyar, Kirsten L. Boedeker, Samuel Brady, Jiahua Fan, Shuai Leng, Kyle J. Myers, et al. 2019. “Performance Evaluation of Computed Tomography Systems: Summary of AAPM Task Group 233.” *Medical Physics* 46 (11): e735–56.

Samei, Ehsan, and Donald J. Peck. 2019. *Hendee’s Physics of Medical Imaging*. *Hendee’s Physics of Medical Imaging*.

Sandfort, Veit, Mark A. Ahlman, Elizabeth C. Jones, Mariana Selwaness, Marcus Y. Chen, Les R. Folio, and David A. Bluemke. 2016. "High Pitch Third Generation Dual-Source CT: Coronary and Cardiac Visualization on Routine Chest CT." *Journal of Cardiovascular Computed Tomography* 10 (4): 282–88.

Shaffiq Said Rahmat, Said Mohd, Muhammad Khalis Abdul Karim, Iza Nurzawani Che Isa, Mohd Amiruddin Abd Rahman, Noramaliza Mohd Noor, and Ng Kwan Hoong. 2020. "Effect of Miscentering and Low-Dose Protocols on Contrast Resolution in Computed Tomography Head Examination." *Computers in Biology and Medicine* 123 (July 2021): 103840.

Toshiba, Medical System. 2012. "AIDR 3D Iterative Reconstruction: Integrated, Automated and Adaptive Dose Reduction." *White Paper*, 1–10.

Verdun, Francis. 2018. "[I120] Image Quality in CT: From Physical Measurements to Model Observers." *Physica Medica* 52 (2018): 46.

Völgyes, David, Marius Pedersen, Arne Stray-Pedersen, Dag Waaler, and Anne Catrine Tregde Martinsen. 2017. "How Different Iterative and Filtered Back Projection Kernels Affect Computed Tomography Numbers and Low Contrast Detectability." *Journal of Computer Assisted Tomography* 41 (1): 75–81.

Webb, S. W., and R. Mark Henkelman. 1990. *Physics of Medical Imaging* . *Physics Today*. Vol. 43.

Weinman, Jason P., David M. Mirsky, Alexandria M. Jensen, and Nicholas V. Stence. 2019. "Dual Energy Head CT to Maintain Image Quality While Reducing Dose in Pediatric Patients." *Clinical Imaging* 55 (February): 83–88.

Yeung, A. W.K. 2019. “The ‘as Low As Reasonably Achievable’ (ALARA) Principle: A Brief Historical Overview and a Bibliometric Analysis of the Most Cited Publications.” *Radioprotection* 54 (2): 103–9.